Gyres, jets and waves in Earth's core

Christopher C. Finlay[1,*], Nicolas Gillet[2], Julien Aubert[3], Philip W. Livermore[4], and Dominique Jault[2]

[1]DTU Space, Technical University of Denmark, Kongens Lyngby, Denmark
[2]Université Grenoble Alpes, Université Savoie Mont Blanc, CNRS, IRD, UGE, F-38000 Grenoble, France
[3]Institut de physique du globe de Paris, CNRS, Université Paris Cité, F-75005 Paris, France.
[4]School of Earth and Environment, University of Leeds, Woodhouse Lane, Leeds LS2 9JT, UK
[*]e-mail: cfinlay@space.dtu.dk

ABSTRACT

Turbulent motions of liquid metal in Earth's outer core generate the geomagnetic field and are responsible for its slow evolution. Electromagnetic, thermal, gravitational, and mechanical processes couple these outer core motions to the inner core and mantle. Twenty years of magnetic field observations from low-earth-orbit satellites, together with advanced numerical simulations, indicate core motions are today dominated by a planetary-scale gyre, a jet in the northern polar region, and waves involving the magnetic field. Here, we review this emerging picture of core dynamics. The planetary gyre is anticyclonic, offset from the rotation axis towards low latitudes under the Atlantic hemisphere, and involves flow speeds of 15-50 km yr^{-1} that are fastest in a focused westward jet under the Bering strait. A Quasi-Geostrophic, Magnetic-Archimedes-Coriolis, force balance likely governs the evolution of such flows on decadal to centennial timescales. Waves in the core flow with periods $\sim$ 7 yrs have been detected at low latitudes using satellite observations, while numerical simulations and theoretical analysis suggest they involve an interplay between Magnetic, Coriolis and inertial effects. These core gyres, jets and waves underlie changes in Earth's magnetic field, and influence other geophysical processes such as Earth's rotation, on interannual to centennial timescales.

Key points:

- Twenty years of satellite observations provide a reliable global picture of how Earth's magnetic field is changing on interannual to decadal timescales. The most intense changes are found at mid-to-low latitudes under the Atlantic hemisphere and also under Alaska and Siberia at high northern latitudes.
- Global knowledge of geomagnetic field changes, together with our understanding of the motional induction process in the core, enable the general circulation of liquid metal in the outer core to be inferred.
- Key features of the core flow include a planetary-scale, eccentric, anticyclonic gyre with an intense jet-like concentration under the Bering strait, and waves at low latitudes.
- Numerical simulations of the geodynamo are now approaching conditions relevant to Earth's core. These demonstrate that a combination of core convection and hydromagnetic waves can produce the observed field variations.
- Changes in the length-of-day on interannual and decadal periods recorded over the past century are well explained by changes in the axisymmetric part of the core flow inferred from geomagnetic observations.

Website summary:
Gyres, jets and waves are thought to play an important role in the dynamics of Earth's core. We review what is known about these processes based on satellite observations and numerical simulations. Implications for deep-Earth coupling mechanisms and forecasting geomagnetic field changes are described.

Introduction

Gyres, jets and waves dominate the dynamics of Earth's outer core[1–7]. The flow of liquid metal in the core is organized by the planet's rotation into columnar or sheet-like circulations known as gyres whose structure is largely invariant parallel to the rotation axis[8–12]. At certain locations these flows can become funnelled into intense jets[13–15]. Outer core flow, including its gyres and jets, advects heat and light material around the core on slow timescales of decades to centuries[16–18]. Waves involving the magnetic field and rotation can communicate disturbances much more rapidly, propagating energy and angular momentum across the core on timescales of days to decades[19–28].

Though deeply hidden, flow patterns in Earth's core, such as gyres, jet and waves, have connections to many parts of the Earth system. Firstly, they control the evolution of Earth's magnetic field, a vital part of our natural environment responsible for deflecting the solar wind and cosmogenic charged particles around Earth[29–35] and providing a suitable habitat for life to flourish. Gyres, jets and waves in the core are central in ongoing efforts to better understand and predict future changes in Earth's magnetic field[36–38]. Changes in the motions of liquid metal in the core also cause changes in Earth's rotation, due to conservation of angular momentum in the coupled Earth system. Core motions can thus produce geodetic signals on interannual to decadal timescales unrelated to solar forcings. There is also an important coupling of core motions to structures in the deep mantle, for example the Large-Low-Shear-Velocity-Provences[39–41], through thermal[42,43], electromagnetic[44], topographic[45] and gravitational[46] mechanisms.

As in the atmosphere and oceans, gyres, jets, and waves in Earth's core are strongly influenced by the planet's rapid rotation[47–49]. However, because it is a good electrical conductor, a strong magnetic field is also present in the core, generated there by a dynamo process that converts the kinetic energy of core motions into magnetic energy[50–52]. Strong magnetic fields allow additional dynamics, including special types of waves involving both magnetic fields and rotation[53–55]. By tracking geomagnetic field changes, it is possible to probe these rich planetary-scale fluid processes taking place in Earth's core.[56–63].

The present working model of core dynamics, involving the key timescales collected in Table 1, may be summarized as follows. Energy is supplied to the system by convective (and possibly also tidal or precessional) forcing[64–66], then subsequently transferred to other scales by the rotating magnetic turbulence including gyres, jets and waves[67]. Due to the rapid rotation flow structures tend to be columnar but this does not indicate a minor role for the magnetic field. A strong, dynamo-generated, magnetic field fundamentally shapes the form of core convection. Intense flows tend to arrange themselves to align their shear with field; as a result flows are on average subject to relatively weak magnetic forces[68–70]. Such alignment can however not hold everywhere, otherwise the dynamo would die. The resulting magnetic tension effects are also crucial in transient core dynamics. Waves are possible due to the rigidity provided by rotation and the magnetic field, and can propagate across the core since dissipative processes are relatively weak on large length scales. At smaller scales energy is lost primarily through Ohmic dissipation[71]. From this complex, driven-dissipative, system gyres, jets and waves emerge to control the observed patterns of geomagnetic field change.

A number of fundamental issues are however not yet well understood. For example the process responsible for producing a coherent planetary-scale gyre, the importance of the region above and below the inner core known as the tangent cylinder in the dynamics, the possible impacts of stratified layers at the top and bottom of the core, and the role of boundary coupling. It is challenging to study these questions both in the laboratory and in numerical simulations due to the vast ranges of spatial and temporal scales involved, and due to difficulties in implementing realistic driving and boundary coupling mechanisms. Observations therefore play a key role in driving progress. A major advance since 1999 has been the availability of high quality satellite observations of the geomagnetic field[72–74]. This has enabled global high resolution studies of the flow in Earth's core[75–77] providing important new insights and constraints on interannual to decadal core dynamics.

In this review we present a synthesis of results from recent observation-based models of the flow in Earth's core and insights obtained from numerical simulations of the core dynamo, focusing on gyres, jets and waves. Models of the core flow derived from magnetic field observations alone are non-unique[59,78,79]. The flow models presented here have been derived using statistical prior information obtained from specific numerical dynamo simulations[17,27,80]. In particular they assume a well-mixed core whose dynamics is dominated by rotation. We note that if there were a stratified layer at the top of the core[81,82], other forms of flow[83,84], involving waves related to the degree of stratification[26,85,86], would be favoured.

We begin by describing the geomagnetic observations which are the basis of our knowledge, and how these are used to infer the core flow. We describe in detail the structure of the planetary gyre, the development of a high latitude jet under Alaska and Siberia, and waves recently detected at low latitudes, comparing these to similar phenomenon found in numerical dynamo simulations. Implications for changes in the length-of-day and for core-mantle coupling processes are discussed. Finally we offer perspectives regarding a route towards operational models of core dynamics that could allow improved forecasts of future geomagnetic field changes.

Variations in Earth's magnetic field

Observed slow variations of Earth's magnetic field are the primary source of our knowledge of core dynamics. In this section we present and discuss maps of the time-dependent core surface field that underlie studies of the core flow.

The core-generated magnetic field and its time changes are today routinely monitored using measurements made by ESA's *Swarm* satellite mission[87,88] (Box 1), complemented by measurements at ground observatories[89–92]. On timescales of years and longer, for which the effects of electrical currents in the poorly conducting mantle are thought to be relatively small, the field and its time variations can be mapped down to the core surface[61,93–96] (Fig. 1(a)). On approaching the field sources in the core the amplitude of the field increases, with maximum values of order 70,000 nT at Earth's surface increasing to order of 1,000,000 nT at the core surface, with the importance of smaller scale features enhanced[97,98]. The core surface field is arranged into bundles of strong flux, including at low latitudes under the Atlantic hemisphere[61,99] and at high latitudes under Canada, Siberia and south of Australia[100,101] (Figure 1(a), for example). We are restricted to knowledge of the long wavelength core surface field because at shorter wavelengths (less than approximately 3000km at Earth's surface) the signal from magnetized rocks in the lithosphere dominates over the core field signal[95,102].

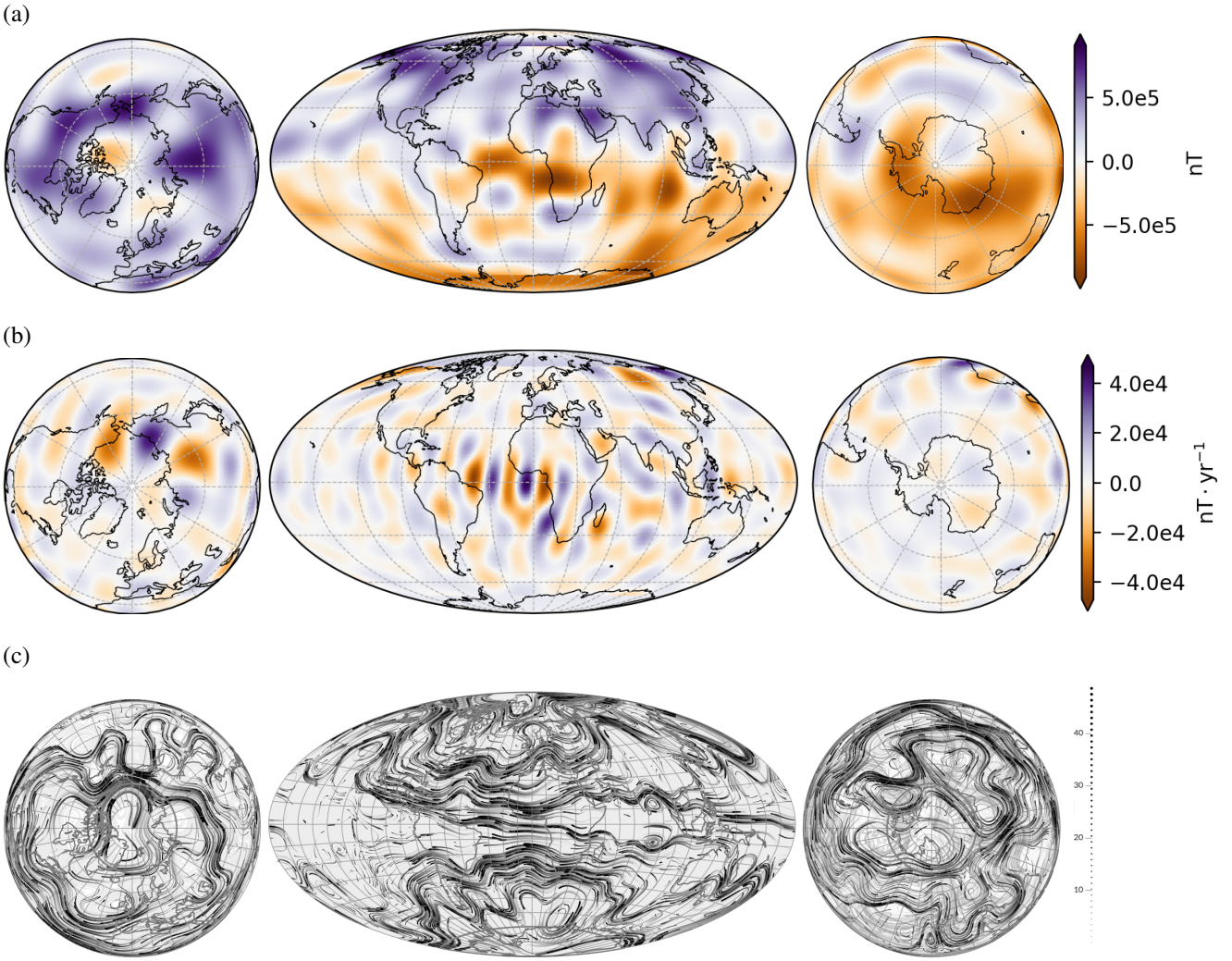

Figure 1. Observed core surface magnetic field and flow in 2020. (a) | Radial magnetic field at the core surface, based on *Swarm* satellite data via the CHAOS-7 field model[91] truncated at spherical harmonic degree 13. **(b)** | Rate of change (secular variation) of the radial magnetic field at the core surface truncated at spherical harmonic degree 17[91]. **(c)** | Streamlines of the core surface flow from the flow model of Gillet et al. (2022)[7] inferred from the CHAOS-7 field model. Line thickness indicates speed, numbers on the scale are in units of km yr^{-1}. Flow direction is westward under the Atlantic hemisphere.

With high quality satellite data, for example from the *Swarm* mission, it is also possible to derive models of the time-derivative (known as the secular variation or SV) of the core surface field. Fig. 1(b) shows the rate of change of the core

surface radial field component in 2020.0 from one such model that has an rms misfit to *Swarm* non-polar vector magnetic field observations of 2.0 nT and to ground observatory SV data of 3.5 nT/yr[91]. It is at present only possible to recover the large-scale core surface SV, up to about spherical harmonic degree 17, although power at higher degrees is expected to add coherently[103,104]. The largest field changes are presently taking place at low latitudes under the Atlantic hemisphere and are associated with westward drift of low latitude flux concentrations[105–107]. At high northern latitudes there is a strong SV signal linked to westward movement of flux under under Alaska, the Bering strait, and Siberia[6,108]. Twenty years of satellite observations now provide a reliable picture of how this large-scale part of Earth's magnetic field changes on interannual to decadal timescales.

An eccentric planetary gyre

We now turn to how core flow patterns are inferred from geomagnetic field changes and discuss Fig. 1(c) which shows map of the core surface flow inferred from *Swarm* satellite observations. The dominant flow pattern found in such maps is the eccentric planetary gyre. In this section we discuss its structure, dynamics and possible origin.

Changes of the core surface magnetic field, including those in Fig. 1(b), are produced by a combination of (i) advection and stretching of the field by core flow, and (ii) diffusion of the field due to the finite conductivity of the core[3,4,16,57]. This process is described mathematically by the magnetic induction equation (see Box 2) which follows from Maxwell's equations, the quasi-static approximation and Ohm's law for a moving conductor[109]. Usually only the radial component of the induction equation is considered at the core surface since the radial field is continuous across boundary layers at the top of the core. Decomposing the radial field into the sum of an observed large-scale part and an unresolved small-scale part, $B_r = \overline{B}_r + \tilde{B}_r$, the radial component of the induction equation is

$$\frac{\partial \overline{B}_r}{\partial t} = -\overline{\nabla_{\mathrm{H}} \cdot (\mathbf{u}\overline{B}_r)} + e, \tag{1}$$

where $\mathbf{u}$ is the core surface flow, $\nabla_H = (\nabla - \frac{\partial}{\partial r}\mathbf{r})$ is the horizontal divergence, and e is an error term that includes the contributions of magnetic diffusion and induction on large scales due to the flow interacting with unresolved small-scale field $-\overline{\nabla_{\mathrm{H}} \cdot (\mathbf{u}\tilde{B}_r)}$. The core surface flow can then be inferred from observed field changes by solving an inverse problem for $\mathbf{u}$ based on (1), given observations of $\overline{B}_r$ and $\frac{\partial \overline{B}_r}{\partial t}$ along with additional assumptions as to the nature of the flow.

Fig. 1(c) shows a map of the flow at the top of the core constructed in this way, based on magnetic field observations made by *Swarm* satellites and at ground observatories[91], combined with a-priori information on the expected flow statistics derived from a specific geodynamo simulation[7,63]. The map shows 1700 randomly distributed tracers following the instantaneous flow in 2020 centered on the Atlantic hemisphere.

Gyre structure

The most prominent feature of the observed core surface flow is a large-scale anticyclonic circulation known as the eccentric planetary gyre[5,63,110,111]. A clear view of the planetary gyre is obtained in Fig. 2(a) by looking down from the north pole, time-averaging the flow over 2000 to 2020 and truncating at spherical harmonic degree 12 to remove small scales.

The planetary gyre flows westwards at mid and low latitudes under the Atlantic hemisphere, consistent with westward drifting patterns of magnetic field observed in this region since the 17th century[112,113] (Fig. 1(c) and 2(a)). Under the Americas the gyre turns poleward, moving in an approximately meridional direction until it reaches high latitudes under the Bering Strait. There it again flows westwards in an intense localized jet, before returning equatorward under Asia.

A cartoon highlighting the key features of the planetary gyre is shown in Fig. 2(b). It is anticyclonic, so it flows in the opposite direction to Earth's rotation, and it is largely symmetric about the equator, especially at mid and low latitudes, see Fig. 1(c). There are however local departures from equatorial symmetry, for example the high latitude jet in the Northern hemisphere is less obvious in the south. The planetary gyre is eccentric in that it is offset from the rotation axis; it flows under the Atlantic hemisphere at mid and low latitudes while under the Pacific hemisphere it is more focused at high latitudes. A series of core flow inversion studies have shown how the planetary gyre can account for much of the decade to century timescale change observed in the geomagnetic field at Earth's surface[5,107,110,111]. Its fluctuations also contribute to changes in the length of day on these timescales[5].

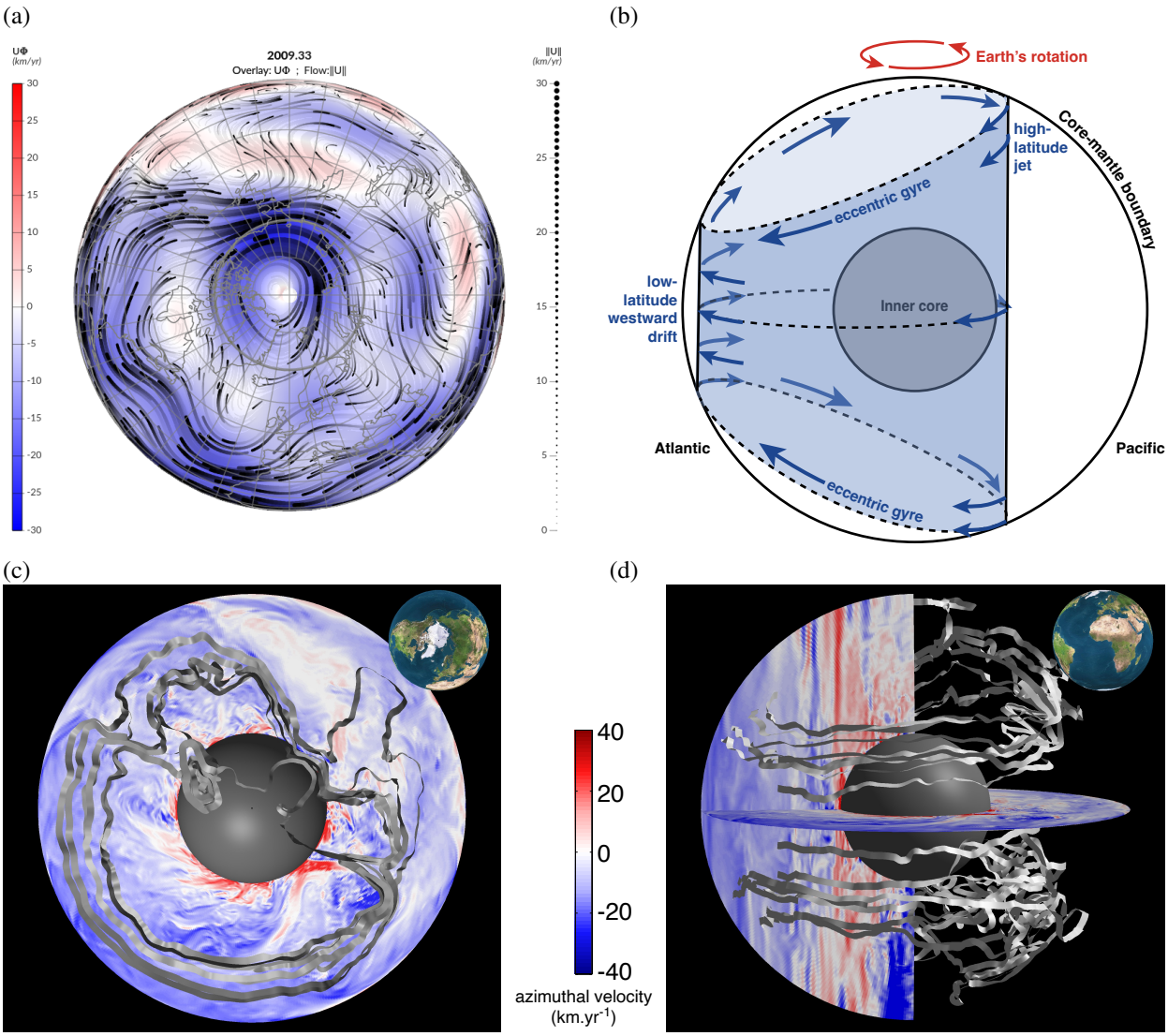

Figure 2. The planetary gyre. (a)| Flow at Earth's core surface, time-averaged between 2000 and 2020 and truncated at degree 12, from Gillet et al (2022)[7] , looking down from the north pole. Black streaks show tracers, colours show the azimuthal flow, blue is westwards. **(b)** | Cartoon of the planetary gyre[27]. **(c)** | Azimuthal flow within outer core from the numerical simulation of Aubert and Gillet (2021)[27] looking down from the north pole. **(d)** | Meridional section from the same simulation. Ribbons trace the path of the eccentric gyre.

No unique solution

It is important to note that core flow reconstructions, such as those shown in Fig. 1(c) and Fig. 2(a) involve assumptions. It is impossible to obtain a unique flow solution based on geomagnetic observations alone since these only provide information on the large-scale part of the magnetic field, and flow inversion schemes are based on a single scalar equation (1), that describes changes in the radial field, while there are two unknown components of the core surface velocity field[59,78]. For example, toroidal flow around isocontours of the core surface radial field produces no change in the radial field[114]. Additional assumptions, based on the physically expected form of flow, are thus necessary[3,4,79,115,116]. Moreover, magnetic diffusion is either neglected (the frozen-flux approximation[57,78]), estimated using empirical relations[117,118], or treated as an error with known statistics based on results from dynamo simulations[63,119,120]. Lack of information on the small-scale field particularly hinders recovery of small scale flow[121–123]. The flow is therefore often assumed to be large scale[124,125] or else the impact of unresolved scales is included as an error term[5,62,63,120]. Despite these challenges there is now considerable agreement across a variety of approaches concerning the planetary-scale flow inferred from satellite observations[62,63,75,76,79,111,117,126]. The planetary gyre structure becomes clearer on time-averaging and if only the large length scale flow is considered. Flow variations on interannual to decadal timescales, especially at low latitudes, also turn out to be particularly well constrained by the observations and show evidence for waves[75–77].

The specific global-scale flow models presented here[7] were derived using a Kalman filter type inversion scheme[63], that relies on spatio-temporal statistics (covariances) of the field and flow, including sub-grid and diffusion effects, taken from a geodynamo simulation[27]. Assumptions regarding the nature of the flow are thus built in, such that these flows are statistically compatible with the flows found in the dynamo simulation, unless the observed secular variation demands otherwise. There are however no strict constraints applied to the flow geometry in this approach, for example flows crossing the equator and departures from equatorial symmetry are allowed. Other flow models, also fitting the observations but compatible with alternative prior information regarding the nature of the flow, are nonetheless certainly possible. For example, if there were a stratified layer at the top of the core[24,81,82], the a-priori spatio-temporal statistics would be different, and there may be changes in some aspects of inferred core flow patterns. Despite this caveat, the flows shown here are notable in that they are consistent both with geomagnetic observations and with advanced simulations of the geodynamo that include many of the basic processes (rotation, convection, hydromagnetic waves) thought to be important in the core.

Gyre dynamics

We now turn to insights gained directly from simulations of the geodynamo (Box 2) which provide dynamically consistent examples of how the planetary gyre can originate and its 3D structure within the core. Fig. 2(c) and (d) show a planetary gyre produced in a version[27] of the coupled-Earth dynamo simulation of Aubert and colleagues[17,80]. The similarity to the observed gyre, with westward flow at low latitudes under the Atlantic hemisphere and approaching the tangent cylinder under the Pacific is striking. Key ingredients for obtaining the gyre in this particular model were (i) gravitational coupling between the inner core and the mantle – this produces generally westward flow with respect to the mantle outside the tangent cylinder because thermal winds inside the tangent cylinder pull the inner core (and therefore by gravitational coupling also the mantle) eastwards –, and (ii) enhanced convective forcing in the Eastern hemisphere at the inner core boundary – this anchors the eccentric structure of the gyre with vigorous upwellings and equatorward motions in the Asian sector with flow returning to high latitudes under the Americas where convective forcing is weaker. A Quasi-Geostrophic, Magnetic-Archimedes-Coriolis (QG-MAC) force balance is found on convective timescales, and at large lengthscales, outside the tangent cylinder[13] in these simulations[49]. It involves an approximate leading order force balance between Coriolis and Pressure effects, with Magnetic, buoyancy (Archimedes) and the remaining Coriolis force entering at the next order[49,80,127] such that

$$\begin{aligned} 2\left(\widehat{\mathbf{z}}\times\mathbf{u}_0\right) &\approx -\nabla P_0 && \text{Quasi-Geostrophic} \\ \underbrace{2\left(\widehat{\mathbf{z}}\times\mathbf{u}'\right)}_{\text{(Ageostrophic) Coriolis}} &\approx -\nabla P' + \underbrace{Ra_F\, C\,\frac{\mathbf{r}}{r_o}}_{\text{Archimedes}} + \underbrace{\left(\nabla\times\mathbf{B}\right)\times\mathbf{B}}_{\text{Magnetic}} && \text{MAC balance} \end{aligned} \tag{2}$$

Here the flow is $\mathbf{u}\approx\mathbf{u}_0+\mathbf{u}'$ and $P\approx P_0+P'$ is a generalized pressure, where subscript 0 represents the leading order force balance and primed variables are departures from this, C is the density anomaly, r_o the core radius, $\widehat{\mathbf{z}}$ is a unit vector along the rotation axis, $\mathbf{r}$ a radial vector, and Ra_F the flux Rayleigh number (see Box 2 for its definition and details of how the equations have been non-dimensionalized).

Lateral variations in the core-mantle boundary conditions, for example due to mantle convection extracting more heat in some locations[42,43] or inhomogeneities in lower mantle electrical conductivity[128] are an alternative mechanism for producing long-lived, systematic, flow differences between the Atlantic and Pacific hemispheres and the planetary gyre. It is also possible that the planetary gyre is a transient fluctuation or instability rather than a long-term feature. Planetary-scale (azimuthal wavenumber $m=1$), long-period, fluctuations have been seen in some turbulent rotating dynamo simulations[13].

One interpretation of these features is that they are long period MC or MAC waves (see glossary for definitions). A suggestion along similar lines is that the gyre may be long-lived MC solitary wave[129]. If the gyre is such a feature it should be understood as a long-period disturbance to the basic state (due to slow waves or nonlinear interactions), rather than a time-averaged feature of core convection due boundary effects. Accurate knowledge of the planetary gyre on century to millenial timescales are needed to distinguish between these scenarios.

A strengthening high latitude jet

A distinctive change in the pattern of secular variation at high northern latitudes between 2000 and 2020 is well explained by a strengthening localized jet of intense westward flow under Alaska and Siberia[6,62,63]. In this section we focus on this high latitude jet, its possible origin, and its relation to the planetary gyre.

Fig. 3(a) presents the observed core surface radial field SV[91] and the inferred core surface flow[7] in 2000 and 2020, focusing on the region below Alaska and Siberia. The high latitude part of the planetary gyre under this region has strengthened and moved westwards[6,62,63] during this period. This flow feature is often referred as a jet[6,62,63] due to its intensity and narrow structure; it provides a simple explanation for high amplitude patches of radial field secular variation and secular acceleration that are observed to have grown in the northern polar region between 2005 and 2015[89,90,107].

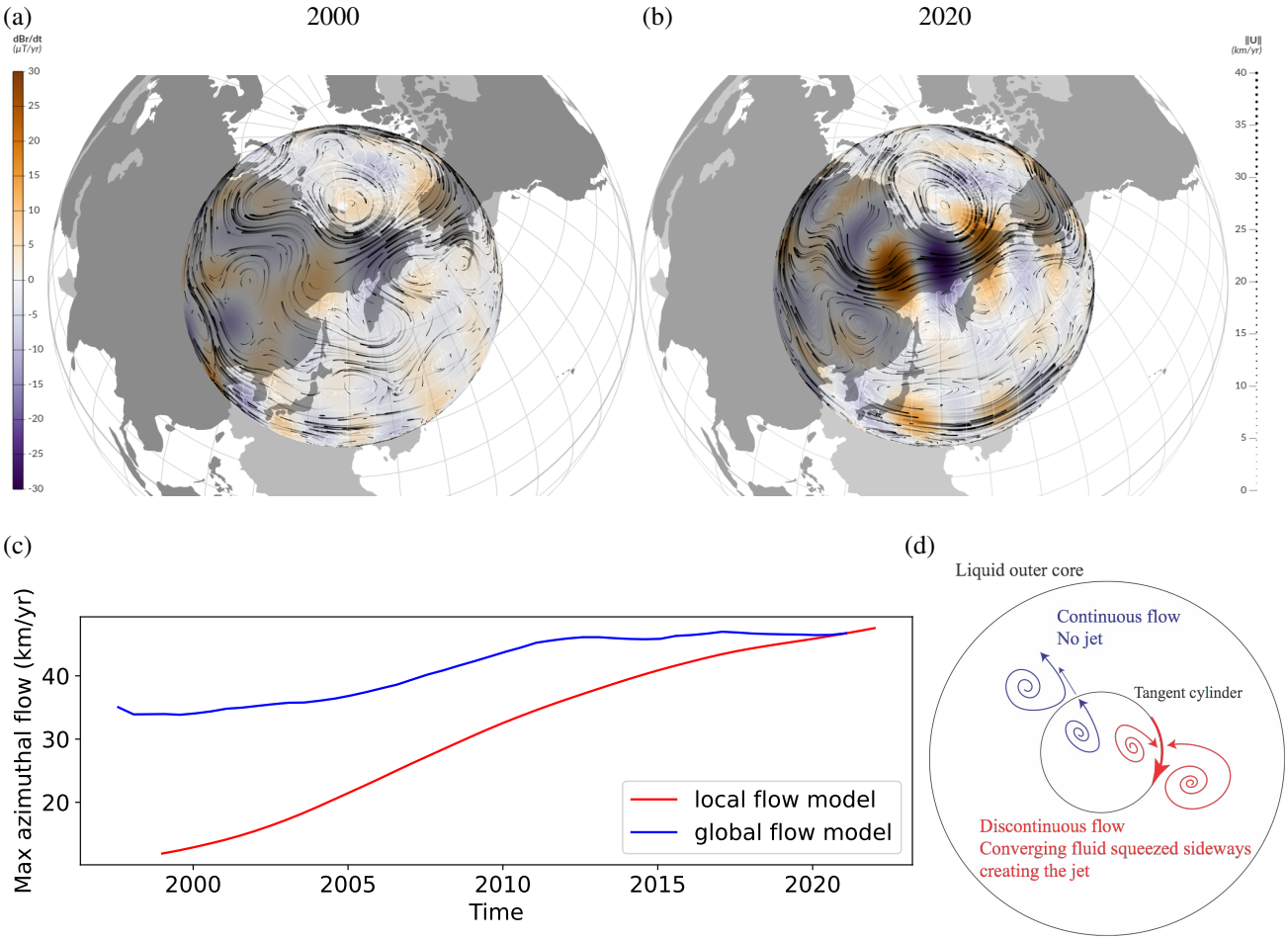

Figure 3. Evolution of the high latitude jet (a) | Model of the CMB Radial field SV[91] (colours) up to degree 16 and an associated core surface flow[7] up to degree 12 shown by black streamlines, in 2000. **(b)** | Similar to (a) but in 2020. **(c)** | Jet strengthening over latitudes $60-80°$N estimated by fitting a simple local flow model[6] to the main field (degree 13) and SV (degree 17) of the CHAOS-7 field model[91] and from a complex global flow model[7]. **(d)** |. Possible mechanism for producing the high latitude jet: discontinuous dynamics across the inner core tangent cylinder can generate an azimuthal jet.

The inferred amplitude of the jet acceleration depends on the adopted flow inversion method; simplified local schemes favour a larger acceleration while global methods that allow more complex flows and account for modelling errors suggest more

modest accelerations[63]. The acceleration estimated by fitting a simplified model[6] is shown in Fig. 3(c), along with predictions from the more complex flow shown in Fig 3(a,b)[7].

It is striking that the high latitude jet occurs very close to the inner core tangent cylinder. This suggests a possible mechanism for the jet formation, illustrated in Fig. 3(d). The tangent cylinder is a dynamical barrier to columnar cylindrical radial motions naturally arising in rapidly rotating spherical dynamos. Inside the tangent cylinder, vigorous convection including large scale vortices occur regularly[130], while outside the tangent cylinder flow consists of sheet like plumes with separate dynamics[13]. Localised gradients in the cylindrical radial flow at the tangent cylinder caused by dynamical imbalance would drive significant lateral flow through mass conservation. Such gradients could also arise when the tangent cylinder acts as a barrier in the cylindrical radial direction, causing the flow to be laterally deflected. Intense, non-axisymmetric, jets are frequently seen close to the inner core tangent cylinder in strongly forced, low viscosity numerical dynamo simulations[13,14,70]. The large shears found on the tangent cylinder can drive instabilities that spawn eddies and trigger waves.

The evolution of the jet over the past two decades seems to be associated with the evolution and meandering of the planetary gyre. The gyre has shifted southward and westwards under North America, and westwards over Siberia, with an associated intensification of the jet under the Bering sea. At the same time there has been a noticeable acceleration of flow in the eastward direction under the low latitude Pacific. The processes within the core driving these changes in both the jet and the gyre are not well understood.

Waves in the core

Next we turn to hydromagnetic waves which are capable of producing rapid dynamics in the core. Such waves are excited in electrically conducting fluids when strong magnetic fields are present, flow crosses the magnetic field lines, and when dissipative processes are sufficiently weak[54,131–133]. We describe observations and inferences of waves in the core surface field and flow, discuss how these can be understood from a theoretical perspective, and how they appear in geodynamo simulations.

Oscillations in the core surface magnetic field and flow

On top of the planetary gyre that dominates the slow general circulation of the core, there is accumulating evidence for waves and oscillations in the core flow on interannual to decadal timescale from satellite observations[5,7,22,74–77,107,126,134–137]. Field oscillations are found, particularly at low latitudes, in the core surface field acceleration[105,106,134,138], or by bandpass filtering to focus on signals with interannual to decadal periods[5,7,22,74,134,137,138]. Initial observations suggested an acceleration pulse[139] and then, as the available time series of satellite data lengthened, an oscillation[108,134] with period about 6 years. Detailed analysis of the field acceleration patterns between 2000 and 2022 is now possible thanks to data from the *Swarm* and earlier CHAMP satellite missions, supplemented by ground observatory[140] and calibrated satellite platform magnetometer data[136,141]. Non-axisymmetric features that drift rapidly in the azimuthal (east-west) direction at low latitudes are evident in time-longitude plots of the field acceleration[136,137,142]. Azimuthal drift speeds of 200 - 1600 km/yr have been reported, depending on the lengthscale and period of the features considered and on the analysis method used[135–137,142]. There is also evidence that field disturbances drift in latitude, for example travelling equatorward at 600 km/yr at 90 degrees east[137]. Such rapid speeds, much faster than the typical advective speeds of 10-50 km/yr found in core flow inversions[3,4,63], suggest a wave origin[135,137,142,143]. Study and interpretation of these signals is however challenging due to the band-limited nature of the accessible signal[38,144]. The field acceleration at the CMB is dominated by short length scales, yet only spherical harmonic degrees up to about degree 10 can be reliably retrieved at present[74,136]. Periods shorter than one year are difficult to access due to challenges in separating magnetospheric, ionospheric and related induced signals[74,145] while only periods shorter than 10 years can be studied with confidence given 20 years of satellite observations.

It turns out to be easier to identify and analyze waves in the core flow, rather than directly in field variations, because the field variations result from complex interactions between wave flows and the spatially varying core field[7]. Torsional waves[2,21], which consist of oscillations in the equatorially symmetric and zonal part of the toroidal flow, are essentially Alfvén waves[131,132], which involve only inertia and magnetic restoring forces, that propagate in the cylindrical radial direction. Such waves with periods around 6 years have been identified in core flows inferred from geomagnetic observations[5,22,77,146]. The identified disturbances tend to propagate outwards from the tangent cylinder toward the equator[22,77]. The observed speed of the torsional waves constrains the strength of the cylindrical radial component of the magnetic field within the core[22,55,147]. A period of about 6 years[22] for the fundamental torsional mode corresponds to a cylindrical radial field of about 2 mT, which suggests a total field strength of about 4 mT assuming an isotropic strength of the three field components in the core. Non-axisymmetric waves have also been detected in the low latitude core flow[5,7,75,76,107,126] from analysis of flow accelerations[75,76,126] or bandpass filtering the flow (to focus on interannual to decadal periods)[5,77]. Non-axisymmetric wave-like motions with periods of roughly 7 years are characterized by velocities of around 5 km yr^{-1} and accelerations around 3 km yr^{-2}, with patterns drifting rapidly in the azimuthal direction at speeds of order 1000 km yr^{-1}, and enhanced in some longitude sectors. For example, disturbances of the azimuthal flow acceleration at longitude 170°E can be followed moving westwards across the Pacific from longitude

130°W, travelling 60° degrees in four years[75]. The result of applying a bandpass filter between 4 and 9.5 years to a core flow model derived from satellite and ground observatory data[7,91] is shown in Fig. 4(a) and (b). The presence of flow oscillations confined to low latitudes is striking, and there is clear evidence for both westward propagation and a wave-like spatio-temporal structure. Being non-axisymmetric these waves carry more information than torsional waves, in particular on longitudinal variations of the magnetic field within the core.

Hydromagnetic wave dynamics

A tentative interpretation of these observed waves in the core, based on a combination of theoretical analysis and numerical simulation studies is as follows, see Figure 4(c) for a visual summary. Hydromagnetic waves result when the background flow, obeying a slowly-evolving QG-MAC balance[49,127], is disrupted, for example by a rapid convective fluctuation[38,143,148]. Due to rapid rotation, the disturbance, which is typically of short wavelength in the cylindrical radial direction, will quickly take on a columnar (quasi-geostrophic) form as energy is rapidly transported in the axial direction by inertial waves[9,25]. When this columnar disturbance moves across the magnetic field, a Lorentz force results, triggering a hydromagnetic wave due to the interplay of inertia and magnetic restoring forces. Such QG Alfvén waves[7,38,143,148] however inevitably feel the Coriolis force through vortex stretching due to the spherical shape of the core. They therefore undergo weak dispersion with larger scale disturbances more strongly affected, especially as they approach the equator where there the column height changes rapidly. By the time they approach the equator their force balance is primarily between magnetic and Coriolis forces so they are then better described as QG MC waves[7,28].

More formally, for columnar disturbances with longer length-scales in the azimuthal than cylindrical radial direction, and for a core magnetic field with azimuthal and cylindrical radial components of similar strength, working in cylindrical polar coordinates (s,ϕ,z), and carrying out a local analysis of a disturbance in terms of plane waves leads to the following dispersion relation[7]

$$\omega = V_A k \left[\left(\frac{k_0}{k}\right)^3 \pm \sqrt{1+\left(\frac{k_0}{k}\right)^6} \right] \tag{3}$$

relating the angular frequency ω and cylindrical radial wavenumber k, where the local Alfvén velocity is

$$V_A(s,\phi) = \sqrt{\frac{1}{2H}\int_{-H}^{H} \frac{1}{\rho\mu_0} B_s^2(s,\phi,z)\,dz} \qquad \text{and} \qquad k_0 = \left(\frac{m\Omega}{V_A H^2}\right)^{1/3},$$

with H being half the height of a fluid column, ρ the fluid density, μ_0 the vacuum magnetic permeability, B_s the cylindrical radial component of the magnetic field, Ω the rotation rate and m the azimuthal wavenumber. Columnar disturbances with very short cylindrical radial wavelengths, with wavenumbers $k > k_0$, are found to essentially follow the dispersion relation for Alfvén waves. For larger cylindrical radial wavelengths, or on approaching the outer boundary where k_0 increases (as H rapidly decreases), then $k < k_0$, and two solutions known as QG inertial (or Rossby) waves and QG MC waves are obtained. Large-scale QG MC waves have periods spanning years to centuries for plausible core field strengths. Sub-decadal periods[28] and a spatial structure focused at low latitudes in agreement with observations[7], are possible provided the disturbance remains of small cylindrical radial extent. QG MC waves are mainly magnetic in the interior, insomuch as their magnetic energy dominates their kinetic energy[28,54]. However their properties at the core-mantle boundary depend on the conductivity of the mantle. Assuming the mantle is insulating, the azimuthal component of the magnetic field is strongly attenuated at the boundary. As a result, the kinetic energy of QG MC waves dominates their magnetic energy at the core-mantle interface, in the same ratio as inferred from the observations[7]. Going beyond the predictions of this simple analytic model, more accurate predictions of mode properties are possible by numerically solving an appropriate eigenvalue problem, given an assumed background state for the magnetic field in the core[28,149]. A cartoon illustrating the properties of QG Alfvén and QG MC waves triggered deep in the core, is shown in Figure 4(c).

It is also possible to investigate such waves in numerical geodynamo simulations. The special class of axisymmetric Alfvén waves known as torsional waves[13,23,150] are easily be isolated due to their structure. Identifying non-axisymmetric hydromagnetic waves is more difficult unless their timescale differs markedly from that of the background convection and rotation[148,151]. Use of hyperviscosity on small length scales of the flow (Box 2) allows simulations with increasingly realistic separations of convective, magnetic (Alfvén) and rotation timescales[27,70,80,143] (Table 1, Box 2). On periods shorter than the convective overturn time but longer than the rotation time, columnar non-axisymmetric hydromagnetic waves (QG Alfvén and QG MC waves) are very obvious in these simulations[27,137,143,148]. Fig. 4(d) presents an example of waves in such a simulation. QG-Alfvén waves are triggered deep in the shell by a convective fluctuation. The disturbance then propagates

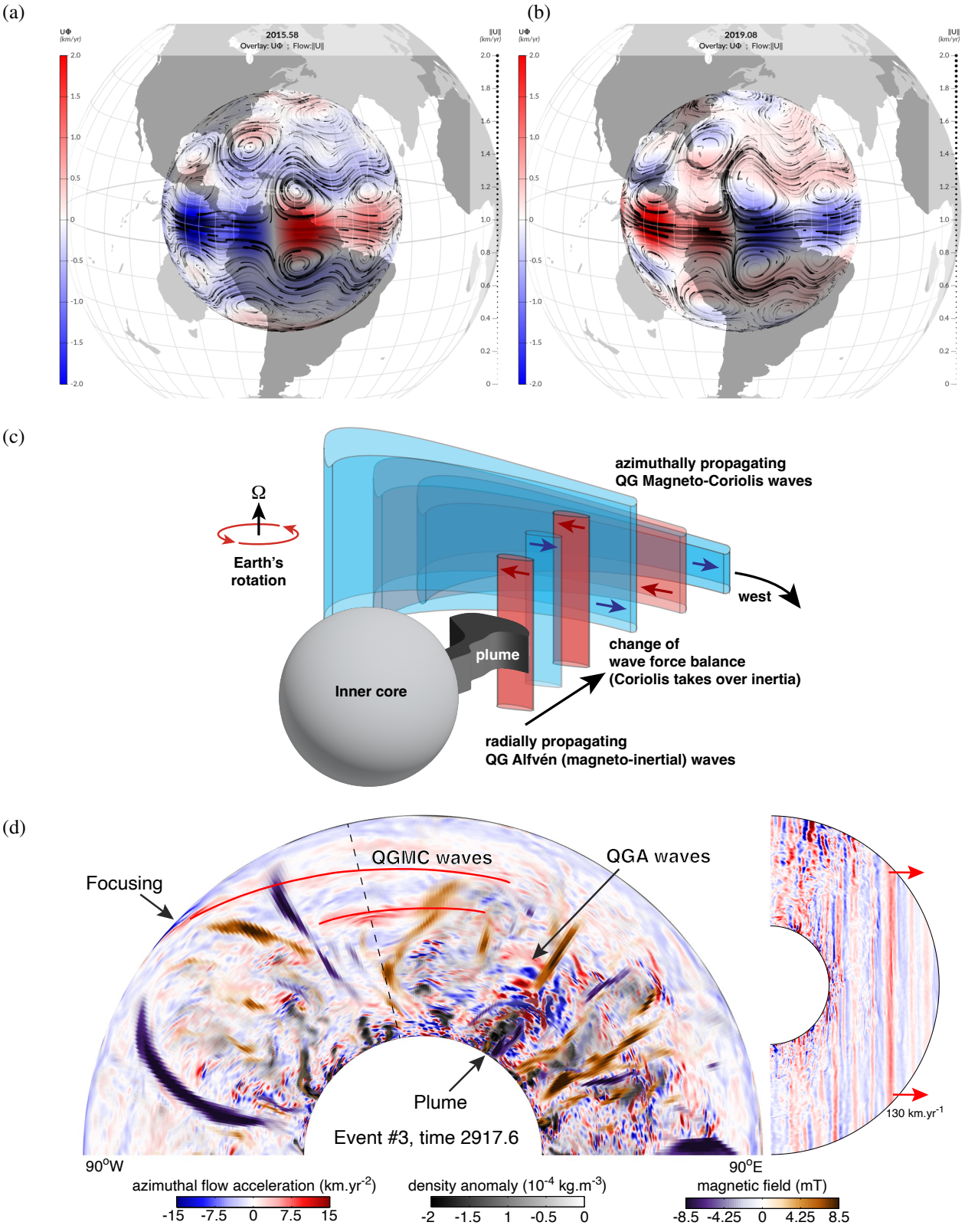

Figure 4. Observed and modelled waves in the core. (a) | A wave disturbance in the core flow inferred from satellite observations, shown in red/blue is the azimuthal (east-west) flow component from a core surface flow model[7] based on the CHAOS-7 field model[91], bandpass filtered between 4 and 9.5 years in 2015.5 **(b)** | in 2019. **(c)** | Cartoon of QG Alfvén and QG MC waves triggered by convection deep within the core. **(d)** | Azimuthal flow acceleration (red/blue) in a snapshot from the simulation of Aubert and Gillet (2021)[27,38], showing the density anomaly (shaded grey) and radial magnetic field (orange/purple) in the equatorial plane (left) and a meridional section (right), during an event where waves were triggered by a convective fluctuation close to the inner core boundary. Red curves locate wave fronts. Reproduced from Aubert et al., (2022)[38].

outwards, becoming more extended, especially in the azimuthal direction, and taking on the character of QG MC waves close to the outer boundary where the column height changes rapidly. Fast changes in the core surface flow and magnetic field acceleration are produced by the waves arriving at low latitudes, reminiscent of patterns in geomagnetic observations[38,143]. In these simulations QG hydromagnetic waves, riding on the basic dynamo state produced by convection, are the origin of sub-decadal secular variation. Considering a simple axisymmetric background magnetic field it is also possible to find MC modes with interannual periods although these seem to involve smaller length scales and considerable magnetic diffusion[149].

Understanding the nature of hydromagnetic waves in the core brings new possibilities, for example variations in propagation speed with location carry information on the structure of the magnetic field within the core, and improved prognostic schemes for predicting future field behaviour become possible. Alternative interpretations of observed oscillations in the geomagnetic field are nonetheless still under debate. For example, MAC waves[24,26,135] are a possibility if a stratified layer exists close to the top of the core. Detailed comparisons of competing wave theories with observations as the satellite record lengthens should help to clarify the situation.

Core-mantle coupling and changes in the Length-Of-Day

Changes in the core flow, including the planetary gyre and the waves described above, can affect the rotation of the Earth[152–154]. This is a consequence of the conservation of angular momentum: an increase in net core angular velocity can only occur with a reduction in the mantle rotation rate with an associated lengthening of the day. Changes in the distribution of angular momentum between the core and mantle occur through their coupling via gravitational, electromagnetic and possibly topographic torques. The dynamics of the core involve periods different to the astronomical forcings (e.g. daily, annual, lunar, solar cycles) which dominate motions in the atmosphere and oceans. In particular the magnetic field strength in the core controls the period of torsional waves that carry angular momentum in the core on interannual timescales[5,22]. QG MC waves can also produce torques on interannual to decadal periods[38,77]. Variations in core convection and the planetary gyre can produce angular momentum fluctuations on timescales of decades to centuries[77,110].

Observed decadal and interannual variations in the length-of-day are well explained by kinematic core flow models inferred from geomagnetic observations[5,77,152,153]. This is important independent evidence that at least the large scale axisymmetric part of the core flow inferred from geomagnetic observations is correct. Comparisons between observed length-of-day variations and predictions from a core flow model[77] are shown in Fig. 5. The agreement both in phase and amplitude is impressive, although not perfect, on both decadal and sub-decadal timescales. Differences can occur, particularly at earlier times, due to issues related to flow non-uniqueness and due to complications with the observations due to the likely leakage of some non-core signals into geomagnetic field models[155].

Distinct periodic signals at approximately 6 years and 8.5 years have recently been reported at interannual to decadal timescales in the LOD time series[156,157]. Filtering core flows around these periods suggests these may be related to interannual QG MC and torsional waves respectively[77]. QG MC waves can contribute to angular momentum changes if the background magnetic field in the core is non-axisymmetric[158,159] and there is suitable core-mantle coupling. Further work is needed to clarify such processes.

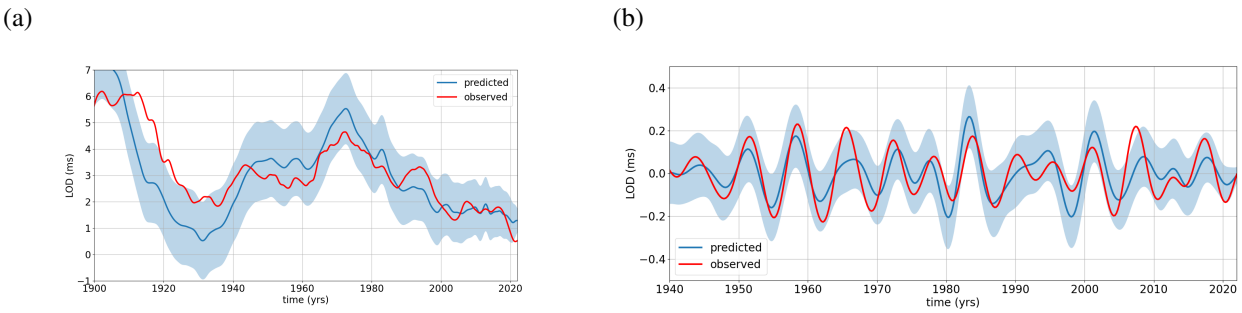

Figure 5. Observed changes in length-of-day (LOD) and predictions from core flows. (a) | Observed change in LOD (red curve), and predicted LOD change from a core flow model[77]. Observed LOD data are derived from Very Long Baseline Interferometry data, from the C04 series[160], with estimated contributions from solid tides (via the IERS 2000 model) and atmospheric angular momentum[161] removed. Blue envelope shows the spread in an ensemble of flow predictions[77]. **(b)** | Band-pass filtered between 4.5 and 9 years.

A dynamical treatment of core motions including core-mantle coupling torques, rather than the traditional kinematic approach, promises to provide additional information on the properties of the lower mantle and upper core. Some numerical

dynamo simulations have already included coupling between the inner core, outer core and mantle[17,38,45,143]. They have demonstrated how hydromagnetic waves arriving at the equator can generate torques and produce inflections in the rate of change of the length of day. In order to perform extensive parameter studies incorporating geomagnetic observations, reduced dynamical models of such processes are needed[162].

Summary and future perspectives

Changes in the Earth's magnetic field, observed in detail over the past two decades by satellites and at ground magnetic observatories, provide global information on the motion of liquid metal in Earth's core. The basic flow circulation at the top of the core is a westwards (anticyclonic) gyre, eccentric with respect to the rotation axis, that reaches low latitudes under the Atlantic hemisphere and closes in the Pacific hemisphere through a focused jet-like flow under the Bering strait, near the inner core tangent cylinder. Numerical simulations suggest the planetary gyre can be understood as a manifestation of QG MAC turbulence with energy input from buoyancy via convection, with organized large scale structures resulting from the strong influence of Coriolis and Lorentz forces, and magnetic dissipation at small length scales[13,14,17]. Fluctuations in the core flow account for decadal and interannual changes in the length-of-day[5,62,77,152,153] that cannot be explained by processes in other fluid envelopes of the Earth system. On interannual to decadal timescales there is mounting evidence that core dynamics is dominated by hydromagnetic waves involving magnetic fields, rotation and fluid inertia, whose properties depend on the wave's lengthscale, period and the location in the core[5,7,77,126,143]. Observed wave patterns at low latitudes agree with the calculated properties of QG MC modes, although other explanations involving possible stratification close to the core surface have been suggested[26,135]. Numerical simulations show such waves can be triggered following local violations of the background QG MAC balance involving fluid inertia, for example due to a convective fluctuation[27,143,148]. Simulations also suggest the arrival of the resultant wave energy at low latitudes at the core surface can account for many of the characteristics of rapid geomagnetic field changes at and above Earth's surface[38,143].

This new picture of rapid core dynamics suggests a path towards dynamically-consistent reduced models of core motions, capable of reproducing satellite magnetic observations and including core-mantle coupling effects. Such models would provide a way to study the physical properties of the core and lower mantle. Structures such as Large-Low-Shear-Velocity-Provinces can affect the properties of hydromagnetic waves in the core. For example, at low latitudes, where the waves have highest amplitude on reaching the core surface, so they can most easily be studied[7,77], wave flows next to regions of high electrical conductivity may be stifled. Given sufficiently long timespans of satellite observations it is possible to envisage performing a hydromagnetic wave tomography of the background flow and magnetic field state within the core. Hydromagnetic waves will also be affected by the thermal state at the top of the core, for example if a stably stratified layer is present. In this way, study of waves in the core might may help to place new constraints on the heat flow currently escaping the core, and, in turn, on Earth's thermal history.

A number of major questions nevertheless remain open. There is no consensus on the origin of the Atlantic-Pacific hemispheric difference, as seen in the eccentric structure of the planetary gyre. Although the gyre appears to be persistent over the past century, which could indicate a long term modulation by lateral variations in the boundary conditions[17], it may also simply be a long-lived transient feature[163], possibly related to longer period MC or MAC waves with a high magnetic to kinetic energy ratio[20,149,151,164,165] with its present eccentric configuration simply a coincidence[13]. It remains unclear what the existence of planetary gyre tells us about the underlying magnetic field and flow within the core and the dynamo process generating it. Numerical simulations show that core motions organize themselves so as to minimize as far as possible flow across magnetic field lines and resultant Lorentz forces[69]; the large-scale core surface flow patterns and the magnetic field within the core would thus appear to be inextricably linked if rotation causes the flow to be invariant along the rotation axis. Maps of the core surface flow show some relatively quiescent regions as well as regions of vigorous flow concentrated along in relatively narrow paths. These structures provide information on the magnetic field within the core and the dynamo process which can be exploited using data assimilation methods together with suitable dynamo simulations[116,166], although obtaining appropriate prior covariances from advanced simulations is at present challenging[167] The CMB field structure may also provide information on zones of regionally confined stratification if these exist[168].

Further advances will depend crucially on securing high quality satellite observations over the long-term. The *Swarm* mission should be extended as far as possible – having multi-decade observations from a single high quality measurement system is essential given the relatively long timescales of core dynamics. Future missions with improved local time coverage, such as the proposed NanoMagsat mission[169] and the Macau Science Satellite-1[170], are needed to go further and unlock the study of high frequency core dynamics which are presently obscured by unwanted ionospheric and induced signals. It should also be a priority to develop more realistic numerical models of hydromagnetic wave dynamics designed to test specific hypotheses, for example related to core field structure, core stratification and core-mantle coupling. At present there are rather few numerical models adapted for such studies.

A perennial question is our ability, or lack of ability, to forecast future changes in the geomagnetic field. This is of

practical importance for users of geomagnetic field models, and is the ultimate test of our understanding of core dynamics. Operational field models (such as the International Geomagnetic Reference Field[171]) today provide forecasts via a simple linear extrapolation, which performs poorly within a few years which requires the reference models to be updated. Such linear extrapolations fail due to oscillations and abrupt changes in the secular variation. In our opinion field forecasts based on dynamical models that correctly capture the relevant wave dynamics, and ingest satellite observations via the tools of data assimilation are clearly the way forward. For this approach to be successful the background state of the magnetic field and flow within the core must first be better determined: this should be a top research priority in the upcoming years.

References

1. Jones, C. 8.05 - Thermal and Compositional Convection in the Outer Core. In Schubert, G. (ed.) *Treatise on Geophysics (Second Edition)*, 115 – 159, DOI: https://doi.org/10.1016/B978-0-444-53802-4.00141-X (Elsevier, 2015), second edition edn.
2. Jault, D. & Finlay, C. C. 8.09 - Waves in the Core and Mechanical Core–Mantle Interactions. In Schubert, G. (ed.) *Treatise on Geophysics (Second Edition)*, 225 – 244, DOI: https://doi.org/10.1016/B978-0-444-53802-4.00150-0 (Elsevier, 2015), second edition edn.
3. Bloxham, J. & Jackson, A. Fluid flow near the surface of Earth's outer core. *Rev. Geophys.* **29**, 97–120, DOI: 10.1029/90RG02470 (1991).
4. Holme, R. 8.04 - large-scale flow in the core. In Schubert, G. (ed.) *Treatise on Geophysics (Second Edition)*, 91 – 113, DOI: https://doi.org/10.1016/B978-0-444-53802-4.00138-X (Elsevier, 2015).
5. Gillet, N., Jault, D. & Finlay, C. C. Planetary gyre, time-dependent eddies, torsional waves, and equatorial jets at the Earth's core surface. *J. Geophys. Res.: Solid Earth* **120**, 3991–4013, DOI: 10.1002/2014jb011786 (2015).
6. Livermore, P. W., Hollerbach, R. & Finlay, C. C. An accelerating high-latitude jet in Earth's core. *Nature Geoscience* **10**, 62–68, DOI: 10.1038/ngeo2859 (2017).
7. Gillet, N. *et al.* Satellite magnetic data reveal interannual waves in Earth's core. *Proc. Natl. Acad. Sci.* **119**, e2115258119, DOI: 10.1073/pnas.211525811 (2022).
8. Busse, F. H. Thermal instabilities in rapidly rotating systems. *J. Fluid. Mech.* **44**, 441–460, DOI: 10.1017/S0022112070001921 (1970).
9. Jault, D. Axial invariance of rapidly varying diffusionless motions in the Earth's core interior. *Phys. Earth Planet. Int.* **166**, 67–76, DOI: 10.1016/j.pepi.2007.11.001 (2008).
10. Davidson, P. A. *Turbulence in Rotating, Stratified and Electrically Conducting Fluids* (Cambridge Univ. Press, Cambridge, 2013).
11. Zhang, K. & Liao, X. *Theory and Modeling of Rotating Fluids* (Cambridge Univ. Press, Cambridge, 2017).
12. Kageyama, A., Miyagoshi, T. & Sato, T. Formation of current coils in geodynamo simulations. *Nature* **454**, 1106–1109, DOI: 10.1038/nature07227 (2008).
13. Schaeffer, N., Jault, D., Nataf, H.-C. & Fournier, A. Turbulent geodynamo simulations: a leap towards Earth's core. *Geophys. J. Int.* **211**, 1–29, DOI: 10.1093/gji/ggx265 (2017).
14. Sheyko, A., Finlay, C., Favre, J. & Jackson, A. Scale separated low viscosity dynamos and dissipation within the Earth's core. *Sci. Rep.* **8**, 12566, DOI: 10.1038/s41598-018-30864-1 (2018).
15. Livermore, P. W. & Hollerbach, R. Successive elimination of shear layers by a hierarchy of constraints in inviscid spherical-shell flows. *J. Math. Phys.* **53**, 073104, DOI: 10.1063/1.4736990 (2012). https://doi.org/10.1063/1.4736990.
16. Elsasser, W. M. The Earth's interior and geomagnetism. *Rev. Mod. Phys.* **22**, 1–35, DOI: 10.1103/RevModPhys.22.1 (1950).
17. Aubert, J., Finlay, C. C. & Fournier, A. Bottom-up control of geomagnetic secular variation by the Earth's inner core. *Nature* **502**, 219–223, DOI: 10.1038/nature12574 (2013).
18. Christensen, U. & Wicht, J. 8.10 - Numerical Dynamo Simulations. In Schubert, G. (ed.) *Treatise on Geophysics (Second Edition)*, 245 – 277, DOI: http://dx.doi.org/10.1016/B978-0-444-53802-4.00145-7 (Elsevier, Oxford, 2015), second edition edn.
19. Braginsky, S. I. Magnetohydrodynamics of the Earth's core. *Geomagn. Aeron.* **7**, 698–712 (1964).

20. Hide, R. Free hydromagnetic oscillations of the Earth's core and the theory of geomagnetic secular variation. *Phil. Trans. R. Soc. Lond. A* **259**, 615–647 (1966).

21. Braginsky, S. I. Torsional magnetohydrodynamic vibrations in the Earth's core and variations in day length. *Geomagn. Aeron.* **10**, 1–8 (1970).

22. Gillet, N., Jault, D., Canet, E. & Fournier, A. Fast torsional waves and strong magnetic field within the Earth's core. *Nature* **465**, 74–77, DOI: 10.1038/nature09010 (2010).

23. Wicht, J. & Christensen, U. R. Torsional oscillations in dynamo simulations. *Geophys. J. Int.* **181**, 1367–1380, DOI: 10.1111/j.1365-246X.2010.04581.x (2010).

24. Braginsky, S. I. Dynamics of the stably stratified ocean at the top of the core. *Phys. Earth Planet. Int.* **111**, 21–34 (1999).

25. Bardsley, O. P. & Davidson, P. A. Inertial–Alfvén waves as columnar helices in planetary cores. *J. Fluid Mech.* **805**, DOI: 10.1017/jfm.2016.577 (2016).

26. Buffett, B. & Matsui, H. Equatorially trapped waves in Earth's core. *Geophys. J. Int.* **218**, 1210–1225 (2019).

27. Aubert, J. & Gillet, N. The interplay of fast waves and slow convection in geodynamo simulations nearing Earth's core conditions. *Geophys. J. Int.* **225**, 1854–1873, DOI: 10.1093/gji/ggab054 (2021).

28. Gerick, F., Jault, D. & Noir, J. Fast Quasi-Geostrophic Magneto-Coriolis Modes in the Earth's Core. *Geophys. Res. Lett.* **48**, e2020GL090803, DOI: https://doi.org/10.1029/2020GL090803 (2021).

29. Glassmeier, K.-H. & Vogt, J. Magnetic Polarity Transitions and Biospheric Effects. *Space Sci. Rev.* **155**, 387—-410, DOI: 10.1007/s11214-010-9659-6 (2010).

30. Channell, J. E. T. & Vigliotti, L. The role of geomagnetic field intensity in late quaternary evolution of humans and large mammals. *Rev. Geophys.* **57**, 709–738, DOI: https://doi.org/10.1029/2018RG000629 (2019). https://agupubs.onlinelibrary.wiley.com/doi/pdf/10.1029/2018RG000629.

31. Masarik, J. & Beer, J. Simulation of particle fluxes and cosmogenic nuclide production in the Earth's atmosphere. *J. Geophys. Res. Atmospheres* **104**, 12099–12111, DOI: https://doi.org/10.1029/1998JD200091 (1999).

32. Dasari, S., Paris, G., Charreau, J. & Savarino, J. Sulfur-isotope anomalies recorded in Antarctic ice cores as a potential proxy for tracing past ozone layer depletion events. *PNAS Nexus* **1**, DOI: 10.1093/pnasnexus/pgac170 (2022).

33. Usoskin, I. G., Korte, M. & Kovaltsov, G. A. Role of centennial geomagnetic changes in local atmospheric ionization. *Geophys. Res. Lett.* **35**, DOI: https://doi.org/10.1029/2007GL033040 (2008).

34. Winkler, H. *et al.* Modeling impacts of geomagnetic field variations on middle atmospheric ozone responses to solar proton events on long timescales. *J. Geophys. Res. Atmospheres* **113**, DOI: https://doi.org/10.1029/2007JD008574 (2008).

35. Gong, F. *et al.* Simulating the solar wind-magnetosphere interaction during the matuyama-brunhes paleomagnetic reversal. *Geophys. Res. Lett.* **49**, e2021GL097340, DOI: https://doi.org/10.1029/2021GL097340 (2022).

36. Aubert, J. Geomagnetic forecasts driven by thermal wind dynamics in the Earth's core. *Geophys. J. Int.* **203**, 1738–1751 (2015).

37. Fournier, A., Aubert, J., Lesur, V. & Ropp, G. A secular variation candidate model for IGRF-13 based on Swarm data and ensemble inverse geodynamo modelling. *Earth, Planets Space* **73**, DOI: 10.1186/s40623-020-01309-9 (2021).

38. Aubert, J., Livermore, P. W., Finlay, C. C., Fournier, A. & Gillet, N. A taxonomy of simulated geomagnetic jerks. *Geophys. J. Int.* **231**, 650–671, DOI: 10.1093/gji/ggac212 (2022).

39. Torsvik, T. H., Smethurst, M. A., Burke, K. & Steinberger, B. Large igneous provinces generated from the margins of the large low-velocity provinces in the deep mantle. *Geophys. J. Int.* **167**, 1447–1460, DOI: 10.1111/j.1365-246X.2006.03158.x (2006).

40. Lay, T. & Garnero, E. J. Deep mantle seismic modeling and imaging. *Annu. Rev. Earth Planet. Sci.* **39**, 91–123, DOI: 10.1146/annurev-earth-040610-133354 (2011).

41. Lay, T. Deep Earth Structure: Lower Mantle and D". In Schubert, G. (ed.) *Treatise on Geophysics (Second Edition)*, 683–723, DOI: https://doi.org/10.1016/B978-0-444-53802-4.00019-1 (Elsevier, Oxford, 2015), second edition edn.

42. Gubbins, D., Willis, A. P. & Sreenivasan, B. Correlation of Earth's magnetic field with lower mantle thermal and seismic structure. *Phys. Earth Planet. Int.* **162**, 256–260 (2007).

43. Mound, J. E. & Davies, C. J. Heat transfer in rapidly rotating convection with heterogeneous thermal boundary conditions. *J. Fluid Mech.* **828**, 601–629, DOI: 10.1017/jfm.2017.539 (2017).

44. Holme, R. Electromagnetic core-mantle coupling - I. Explaining decadal changes in the length of day. *Geophys. J. Int.* **132**, 167–180 (1998).

45. Kuang, W. & Chao, B. F. Topographic core-mantle coupling in geodynamo modeling. *Geophys. Res. Lett.* **28**, 1871–1874, DOI: https://doi.org/10.1029/2000GL012237 (2001).

46. Buffett, B. A. Gravitaional oscillations in the length of day. *Geophys. Res. Lett.* **23**, 2279–2282 (1996).

47. Hide, R. The hydrodynamics of the Earth's core. *Phys. Chem. Earth* **1**, 94–137, DOI: https://doi.org/10.1016/0079-1946(56)90007-6 (1956).

48. Gillet, N., Schaeffer, N. & Jault, D. Rationale and geophysical evidence for quasi-geostrophic rapid dynamics within the Earth's outer core. *Phys. Earth Planet. Int.* **187**, 380–390, DOI: https://doi.org/10.1016/j.pepi.2011.01.005 (2011).

49. Schwaiger, T., Gastine, T. & Aubert, J. Force balance in numerical geodynamo simulations: a systematic study. *Geophys. J. Int.* **219**, S101–S114 (2019).

50. Roberts, P. H. & King, E. M. On the genesis of the Earth's magnetism. *Reports on Prog. Phys.* **76**, 096801, DOI: 10.1088/0034-4885/76/9/096801 (2013).

51. Jones, C. A. Planetary magnetic fields and fluid dynamos. *Annu. Rev. Fluid Mech.* **43**, 583–614, DOI: 10.1146/annurev-fluid-122109-160727 (2011). https://doi.org/10.1146/annurev-fluid-122109-160727.

52. Moffatt, K. & Dormy, E. *Self-exciting fluid dynamos* (Cambridge Univ. Press, Cambridge, 2019).

53. Lehnert, B. Magnetohydrodynamic waves under the action of the coriolis force. *Astrophys. J.* **119**, 647–654 (1954).

54. Acheson, D. J. & Hide, R. Hydromagnetics of rotating fluids. *Reports Prog. Phys.* **36**, 159–221 (1973).

55. Braginsky, S. I. Short-period geomagnetic secular variation. *Geophys. Astrophys. Fluid Dyn.* **30**, 1–78, DOI: 10.1080/03091928408210077 (1984).

56. Bullard, E. The secular change in the Earth's magnetic field. *Mon. Not. Roy. Astr. Soc., Geophys. Suppl.* **5**, 248–257, DOI: https://doi.org/10.1111/j.1365-246X.1948.tb02940.x (1948).

57. Roberts, P. H. & Scott, S. On the analysis of the secular variation — 1 : A hydromagnetic constraint. *J. Geomagn. Geoelectr.* **17**, 137–151 (1965).

58. Kahle, A. B., Vestine, E. H. & Ball, R. H. Estimated surface motions of the Earth's core. *J. Geophys. Res. (1896-1977)* **72**, 1095–1108, DOI: https://doi.org/10.1029/JZ072i003p01095 (1967).

59. Backus, G. Kinematics of geomagnetic secular variation in a perfectly conducting core. *Phil. Trans. R. Soc. Lond. A* **263**, 239–266 (1968).

60. Le Mouël, J., Gire, C. & Madden, T. Motions at core surface in the geostrophic approximation. *Phys. Earth Planet. Int.* **39**, 270–287 (1985).

61. Bloxham, J., Gubbins, D. & Jackson, A. Geomagnetic secular variation. *Phil. Trans. R. Soc. Lond. A* **329**, 415–502 (1989).

62. Bärenzung, J., Holschneider, M., Wicht, J., Sanchez, S. & Lesur, V. Modeling and predicting the short-term evolution of the geomagnetic field. *J. Geophys. Res.: Solid Earth* **123**, 4539–4560, DOI: https://doi.org/10.1029/2017JB015115 (2018).

63. Gillet, N., Huder, L. & Aubert, J. A reduced stochastic model of core surface dynamics based on geodynamo simulations. *Geophys. J. Int.* **219**, 522–539, DOI: 10.1093/gji/ggz313 (2019).

64. Nimmo, F. 8.02 - energetics of the core. In Schubert, G. (ed.) *Treatise on Geophysics (Second Edition)*, 27–55, DOI: https://doi.org/10.1016/B978-0-444-53802-4.00139-1 (Elsevier, Oxford, 2015), second edition edn.

65. Le Bars, M. *et al.* Fluid Dynamics Experiments for Planetary Interiors. *Surv. Geophys.* **43**, 229–261, DOI: 10.1007/s10712-021-09681-1 (2022).

66. Landeau, M., Fournier, A., Nataf, H.-C., Cébron, D. & Schaeffer, N. Sustaining Earth's magnetic dynamo. *Nat. Rev. Earth Environ.* **3**, 255–269, DOI: 10.1038/s43017-022-00264-1 (2022).

67. Nataf, H.-C. & Schaeffer, N. Turbulence in the core. In *Treatise on Geophysics*, 161–181, DOI: 10.1016/b978-0-444-53802-4.00142-1 (Elsevier BV, 2015).

68. Ferraro, V. C. A. The non-uniform rotation of the sun and its magnetic field. *Month. Not. Roy. Astr. Soc.* **97**, 458 (1937).

69. Aubert, J. Steady zonal flows in spherical shell dynamos. *J. Fluid. Mech.* **542**, 53–67 (2005).

70. Aubert, J. Approaching Earth's core conditions in high-resolution geodynamo simulations. *Geophys. J. Int.* **219**, S137–S151, DOI: 10.1093/gji/ggz232 (2019).

71. Christensen, U. & Tilgner, A. Power requirement of the geodynamo from ohmic losses in numerical and laboratory dynamos. *Nature* **429**, 169–171 (2004). Doi: 10.1038/nature02508.

72. Olsen, N. & Stolle, C. Satellite geomagnetism. *Annu. Rev. Earth Planet. Sci.* **40**, 441–465 (2012).

73. Hulot, G., Sabaka, T. J., Olsen, N. & Fournier, A. The present and future geomagnetic field. In *Treatise on Geophysics (Second Edition)*, vol. 5 - Geomagnetism, 33–78 (Elsevier, 2015).

74. Lesur, V., Gillet, N., Hammer, M. & Mandea, M. Rapid variations of Earth's core magnetic field. *Surv. geophysics* DOI: 10.1007/s10712-021-09662-4 (2022).

75. Whaler, K. A., Hammer, M. D., Finlay, C. & Olsen, N. Core surface flow changes associated with the 2017 pacific geomagnetic jerk. *Geophys. Res. Lett.* **49**, e2022GL098616, DOI: 10.1029/2022GL098616 (2022).

76. Ropp, G. & Lesur, V. Mid-latitude and equatorial core surface flow variations derived from observatory and satellite magnetic data. *Geophys. J. Int.* DOI: 10.1093/gji/ggad113 (2023). Ggad113, https://academic.oup.com/gji/advance-article-pdf/doi/10.1093/gji/ggad113/49525063/ggad113.pdf.

77. Istas, M., Gillet, N., Finlay, C., Hammer, M. & Huder, L. Transient core surface dynamics from ground and satellite geomagnetic data. *Geophys. J. Int.* **233**, 1890–1915, DOI: https://doi-org.insu.bib.cnrs.fr/10.1093/gji/ggad039 (2023).

78. Gubbins, D. & Roberts, P. H. Magnetohydrodynamics of the Earth's core. *Geomagn. Ed. Jacobs, J.A.* **2**, 1–183 (1987).

79. Schwaiger, T., Jault, D., Gillet, N., Schaeffer, N. & Mandea, M. Local estimation of quasi-geostrophic flows in Earth's core. *Geophys. J. Int.* **ggad089**, DOI: 10.1093/gji/ggad089 (2023).

80. Aubert, J., Gastine, T. & Fournier, A. Spherical convective dynamos in the rapidly rotating asymptotic regime. *J. Fluid. Mech.* **813**, 558–593, DOI: 10.1017/jfm.2016.789 (2017).

81. Gubbins, D., Thomson, C. & Whaler, K. Stable regions in the earth's liquid core. *Geophys. J. Royal Astron. Soc.* **68**, 241 – 251, DOI: 10.1111/j.1365-246X.1982.tb06972.x (1982).

82. Lister, J. R. & Buffett, B. A. Stratification of the outer core at the core-mantle boundary. *Phys. Earth Planet. Interiors* **105**, 5–19, DOI: https://doi.org/10.1016/S0031-9201(97)00082-4 (1998).

83. Takehiro, S. & Lister, J. R. Penetration of columnar convection into an outer stably stratified layer in rapidly rotating spherical fluid shells. *Earth Planet. Sci. Lett.* **187**, 357–366, DOI: https://doi.org/10.1016/S0012-821X(01)00283-7 (2001).

84. Gastine, T., Aubert, J. & Fournier, A. Dynamo-based limit to the extent of a stable layer atop Earth's core. *Geophys. J. Int.* **222**, 1433–1448, DOI: 10.1093/gji/ggaa250 (2020).

85. Buffett, B. A. Geomagnetic fluctuations reveal stable stratification at the top of the earth's core. *Nature* **507**, 484–487, DOI: 10.1038/nature13122 (2014).

86. Buffett, B. A., Knezek, N. & Holme, R. Evidence for MAC waves at the top of Earth's core and implications for variations in length of day. *Geophys. J. Int.* **204**, 1789–1800, DOI: 10.1093/gji/ggv552 (2016).

87. Friis-Christensen, E., Lühr, H. & Hulot, G. Swarm: A constellation to study the Earth's magnetic field. *Earth, planets space* **58**, 351–358 (2006).

88. Olsen, N. & Floberghagen, R. Exploring Geospace from Space: the Swarm Satellite Constellation Mission. *Space Res. Today* **203**, 61–71, DOI: 10.1016/j.srt.2018.11.017 (2018).

89. Sabaka, T. J., Tøffner-Clausen, L., Olsen, N. & Finlay, C. C. CM6: A comprehensive geomagnetic field model derived from both champ and swarm satellite observations. *Earth, Planets Space* **72**, 80, DOI: 10.1186/s40623-020-01210-5 (2020).

90. Ropp, G., Lesur, V., Baerenzung, J. & Holschneider, M. Sequential modelling of the Earth's core magnetic field. *Earth, Planets Space* **72**, 153, DOI: 10.1186/s40623-020-01230-1 (2020).

91. Finlay, C. C., Kloss, C., Olsen, N., Hammer, M. D. & Tøffner-Clausen, L. The CHAOS-7 geomagnetic field model and observed changes in the South Atlantic Anomaly. *Earth, Planets Space* **72**, DOI: 10.1186/s40623-020-01252-9 (2020).

92. Baerenzung, J., Holschneider, M., Saynish-Wagner, J. & Thomas, M. Kalmag: a high spatio-temporal model of the geomagnetic feld. *Earth, Planets Space* **74**, 139 (2022).

93. Benton, E. R. & Whaler, K. A. Rapid diffusion of poloidal geomagnetic field field through the weakly conducting mantle: a perturbation solution. *Geophys. J. R. Astr. Soc.* **75**, 77–100 (1983).

94. Hagedoorn, J. M. & Martinec, Z. The adjoint-state method for the downward continuation of the geomagnetic field. *Geophys. J. Int.* **201**, 724–740, DOI: 10.1093/gji/ggv049 (2015).

95. Lowes, F. J. Spatial power spectrum of the main geomagnetic field, and extrapolation to the core. *Geophys. J. R. Astr. Soc.* **36**, 717–730 (1974).

96. Risbo, T. Jordens magnetfelt, et uløst hydrodynamisk problem. *Gamma, tidsskrift for fysik, Niels Bohr Institutet* **50**, 21–40 (1982).

97. Shure, L., Parker, R. L. & Langel, R. A. A preliminary harmonic spline model from Magsat data. *J. Geophys. Res.* **90**, 11505–11512 (1985).

98. Gubbins, D. & Bloxham, J. Geomagnetic field analysis- III. Magnetic fields on the core-mantle boundary. *Geophys. J. R. Astr. Soc.* **80**, 695–713 (1985).

99. Jackson, A. Intense equatorial flux spots on the surface of Earth's core. *Nature* **424**, 760–763 (2003).

100. Bloxham, J. & Gubbins, D. The secular variation of Earth's magnetic field. *Nature* **317**, 777–781 (1985).

101. Gubbins, D. & Bloxham, J. Morphology of the geomagnetic field and implications for the geodynamo. *Nature* **325**, 509–511 (1987).

102. Langel, R. A. & Estes, R. H. A geomagnetic field spectrum. *Geophys. Res. Lett.* **9**, 250–253, DOI: https://doi.org/10.1029/GL009i004p00250 (1982).

103. Holme, R., Olsen, N. & Bairstow, F. Mapping geomagnetic secular variation at the core–mantle boundary. *Geophys. J. Int.* **186**, 521–528, DOI: 10.1111/j.1365-246X.2011.05066.x (2011).

104. Aubert, J. Recent geomagnetic variations and the force balance in Earth's core. *Geophys. J. Int.* **221**, 378–393, DOI: 10.1093/gji/ggaa007 (2020).

105. Lesur, V., Wardinski, I., Rother, M. & Mandea, M. GRIMM: the GFZ Reference Internal Magnetic Model based on vector satellite and observatory data. *Geophys. J. Int.* **173**, 382–394 (2008).

106. Olsen, N., Mandea, M., Sabaka, T. J. & Tøffner-Clausen, L. CHAOS-2 – A Geomagnetic Field Model Derived from one Decade of Continuous Satellite Data. *Geophys. J. Int.* **179**, 1477–1487, DOI: 10.1111/j.1365-246X.2009.04386.x (2009).

107. Finlay, C. C., Olsen, N., Kotsiaros, S., Gillet, N. & Tøffner-Clausen, L. Recent geomagnetic secular variation from Swarm and ground observatories as estimated in the CHAOS-6 geomagnetic field model. *Earth, Planets Space* **68**, DOI: 10.1186/s40623-016-0486-1 (2016).

108. Olsen, N. *et al.* The CHAOS-4 geomagnetic field model. *Geophys. J. Int.* **197**, 815–827 (2014).

109. Alboussière, T. Fundamentals of MHD. In Cardin, P. & Cugliandolo, L. (eds.) *Dynamos*, vol. 88 of *Les Houches*, 1–44, DOI: https://doi.org/10.1016/S0924-8099(08)80005-4 (Elsevier, 2008).

110. Pais, M. A. & Jault, D. Quasi-geostrophic flows responsible for the secular variation of the Earth's magnetic field. *Geophys. J. Int.* **173**, 421–443 (2008).

111. Pais, M. A., Morozova, A. L. & Schaeffer, N. Variability modes in core flows inverted from geomagnetic field models. *Geophys. J. Int.* **200**, 402–420 (2014).

112. Halley, E. A theory of the variation of the magnetic compass. *Phil. Trans. R. Soc. Lond.* **13**, 208–221 (1683).

113. Jackson, A., Jonkers, A. R. T. & Walker, M. R. Four centuries of geomagnetic secular variation from historical records. *Phil. Trans. R. Soc. Lond. A* **358**, 957–990 (2000).

114. Lloyd, D. & Gubbins, D. Toroidal fluid motion at the top of the Earth's core. *Geophys. J. Int.* **100**, 455–467 (1990).

115. Backus, G. E. & Mouël, J.-L. L. The region on the core—mantle boundary where a geostrophic velocity field can be determined from frozen-flux magnetic data. *Geophys. J. Int.* **85**, 617–628 (1986).

116. Aubert, J. Earth's core internal dynamics 1840–2010 imaged by inverse geodynamo modelling. *Geophys. J. Int.* **197**, 1321–1334 (2014).

117. Holme, R. & Olsen, N. Core surface flow modelling from high-resolution secular variation. *Geophys. J. Int.* **166**, 518–528, DOI: 10.1111/j.1365-246X.2006.03033.x (2006).

118. Amit, H. & Christensen, U. R. Accounting for magnetic diffusion in core flow inversions from geomagnetic secular variation. *Geophys. J. Int.* **175**, 913–924 (2008).

119. Barrois, O., Hammer, M. D., Finlay, C. C., Martin, Y. & Gillet, N. Assimilation of ground and satellite magnetic measurements: inference of core surface magnetic and velocity field changes. *Geophys. J. Int.* **215**, 695–712 (2018).

120. Barrois, O. *et al.* Erratum: 'Contributions to the geomagnetic secular variation from a reanalysis of core surface dynamics' and 'Assimilation of ground and satellite magnetic measurements: inference of core surface magnetic and velocity field changes'. *Geophys. J. Int.* **216**, 2106–2113, DOI: 10.1093/gji/ggy471 (2018).

121. Hulot, G., Le Mouël, J.-L. & Wahr, J. Taking into account truncation problems and geomagnetic model accuracy in assessing computed flows at the core—mantle boundary. *Geophys. J. Int.* **108**, 224–246 (1992).

122. Rau, S., Christensen, U., Jackson, A. & Wicht, J. Core flow inversion tested with numerical dynamo models. *Geophys. J. Int.* **141**, 485–497 (2000).

123. Eymin, C. & Hulot, G. On core surface flows inferred from satellite magnetic data. *Phys. Earth Planet. Interiors* **152**, 200–220 (2005).

124. Bloxham, J. The determination of fluid flow at the core surface from geomagnetic observations. In Vlaar, N. J., Nolet, G., Wortel, M. J. R. & Cloetingh, S. A. P. L. (eds.) *Mathematical Geophysics, A Survey of Recent Developments in Seismology and Geodynamics*, 189–208 (Reidel, Dordrecht, 1988).

125. Whaler, K. A., Olsen, N. & Finlay, C. C. Decadal variability in core surface flows deduced from geomagnetic observatory monthly means. *Geophys. J. Int.* **207**, 228–243 (2016).

126. Kloss, C. & Finlay, C. C. Time-dependent low-latitude core flow and geomagnetic field acceleration pulses. *Geophys. J. Int.* **217**, 140–168, DOI: 10.1093/gji/ggy545 (2019).

127. Davidson, P. A. Scaling laws for planetary dynamos. *Geophys. J. Int.* **195**, 67–74, DOI: 10.1093/gji/ggt167 (2013).

128. Dumberry, M. & More, C. Weak magnetic field changes over the pacific due to high conductance in lowermost mantle. *Nat. Geosci.* **13**, 516–520, DOI: 10.1038/s41561-020-0589-y (2020).

129. Hori, K., Tobias, S. M. & Jones, C. A. Solitary magnetostrophic rossby waves in spherical shells. *J. Fluid Mech.* **904**, R3, DOI: 10.1017/jfm.2020.743 (2020).

130. Aurnou, J., Andreadis, S., Zhu, L. & Olson, P. Experiments on convection in Earth's core tangent cylinder. *Earth Planet. Sci. Lett.* **212**, 119–134, DOI: 10.1016/S0012-821X(03)00237-1 (2003).

131. Alfvén, H. Existence of EM-hydrodynamic waves. *Nature* **150**, 405–406 (1942).

132. Davidson, P. A. *An introduction to magnetohydrodynamics* (Cambridge Univ. Press, Cambridge, 2010).

133. Finlay, C. C. Waves in the presence of magnetic fields, rotation and convection. In Cardin, P. & Cugliandolo, L. F. (eds.) *Lecture notes on Les Houches Summer School: Dynamos*, vol. 88, chap. 8, 403–450, DOI: https://doi.org/10.1016/S0924-8099(08)80012-1 (Elsevier, 2008).

134. Chulliat, A. & Maus, S. Geomagnetic secular acceleration, jerks, and a localized standing wave at the core surface from 2000 to 2010. *J. Geophys. Res.* **119**, 1531–1543, DOI: 10.1002/2013JB010604 (2014).

135. Chi-Durán, R., Avery, M. S., Knezek, N. & Buffett, B. A. Decomposition of geomagnetic secular acceleration into traveling waves using complex empirical orthogonal functions. *Geophys. Res. Lett.* **47**, e2020GL087940, DOI: 10.1029/2020GL087940 (2020).

136. Hammer, M. D., Finlay, C. C. & Olsen, N. Applications for cryosat-2 satellite magnetic data in studies of Earth's core field variations. *Earth Planets Space* **73**, 73, DOI: 10.1186/s40623-021-01365-9 (2021).

137. Gillet, N., Gerick, F., Angappan, R. & Jault, D. A dynamical prospective on interannual geomagnetic field changes. *Surv. Geophys.* DOI: 10.1007/s10712-021-09664-2 (2021). Doi: 10.1007/s10712-021-09664-2.

138. Finlay, C. C., Olsen, N. & Toffner-Clausen, L. DTU candidate field models for IGRF-12 and the CHAOS-5 geomagnetic field model. *Earth. Planets. Space.* **67**, 114 (2015).

139. Chulliat, A., Thébault, E. & Hulot, G. Core field acceleration pulse as a common cause of the 2003 and 2007 geomagnetic jerks,. *Geophys. Res. Lett.* **37**, DOI: 10.1029/2009GL042019 (2010).

140. Macmillan, S. & Olsen, N. Observatory data and the Swarm mission. *Earth, Planets Space* **65**, 1355–1362 (2013).

141. Olsen, N., Albini, G., Bouffard, J., Parrinello, T. & Tøffner-Clausen, L. Magnetic observations from CryoSat-2: calibration and processing of satellite platform magnetometer data. *Earth, Planets Space* **72**, DOI: 10.1186/s40623-020-01171-9 (2020).

142. Chulliat, A., Alken, P. & Maus, S. Fast equatorial waves propagating at the top of the Earth's core. *Geophys. Res. Lett.* **42**, 3321–3329, DOI: https://doi.org/10.1002/2015GL064067 (2015).

143. Aubert, J. & Finlay, C. C. Geomagnetic jerks and rapid hydromagnetic waves focusing at Earth's core surface. *Nat. Geosci.* **12**, 393–398 (2019).

144. Gillet, N. Spatial and temporal changes of the geomagnetic field : insights from forward and inverse core field models. In Mandea, M., Korte, M., Petrovsky, E. & Yau, A. (eds.) *Geomagnetism, Aeronomy and Space Weather : a Journey from the Earth's Core to the Sun*, chap. 9 (International Association of Geomagnetism and Aeronomy, 2019).

145. Kloss, C. *Geomagnetic field modelling and polar ionospheric currents*. Ph.D. thesis, Ph. D. thesis, Technical University of Denmark (2021).

146. Gillet, N., Jault, D. & Canet, E. Excitation of travelling torsional normal modes in an Earth's core model. *Geophys. J. Int.* **210**, 1503–1516, DOI: 10.1093/gji/ggx237 (2017).

147. Zatman, S. & Bloxham, J. Torsional oscillations and the magnetic field within the Earth's core. *Nature* **388**, 760–763 (1997).

148. Aubert, J. Geomagnetic acceleration and rapid hydromagnetic wave dynamics in advanced numerical simulations of the geodynamo. *Geophys. J. Int.* **214**, 531–547, DOI: 10.1093/gji/ggy161 (2018).

149. Luo, J., Marti, P. & Jackson, A. Waves in the Earth's core. II. Magneto-Coriolis modes. *Proc. Royal Soc. A: Math. Phys. Eng. Sci.* **478**, 20220108, DOI: 10.1098/rspa.2022.0108 (2022).

150. Teed, R. J., Jones, C. A. & Tobias, S. M. The dynamics and excitation of torsional waves in geodynamo simulations. *Geophys. J. Int.* **196**, 724–735, DOI: 10.1093/gji/ggt432 (2014).

151. Hori, K., Teed, R. & Jones, C. The dynamics of magnetic rossby waves in spherical dynamo simulations: A signature of strong-field dynamos? *Phys. Earth Planet. Interiors* **276**, 68–85, DOI: https://doi.org/10.1016/j.pepi.2017.07.008 (2018). Special Issue:15th SEDI conference.

152. Jault, D., Gire, C. & Le Mouël, J. L. Westward drift, core motions and exchanges of angular momentum between core and mantle. *Nature* **333**, 353–356 (1988).

153. Jackson, A., Bloxham, J. & Gubbins, D. Time-dependent flow at the core suface and conservation of angular momentum in the coupled core-mantle system. *Dyn. Earth's Deep. Interior Earth Rotation, Geophys. Monogr.* **72**, 97–107 (1993).

154. Triana, S. *et al.* Core Eigenmodes and their Impact on the Earth's Rotation. *Surv. Geophys.* **43**, 107–148, DOI: 10.1007/s10712-021-09668-y (2022).

155. Finlay, C. C. *et al.* Challenges handling magnetospheric and ionospheric signals in internal geomagnetic field modelling. *Space Sci. Rev.* **206**, 157, DOI: 10.1007/s11214-016-0285-9 (2017).

156. Duan, P. & Huang, C. Intradecadal variations in length of day and their correspondence with geomagnetic jerks. *Nat. Commun.* **11**, 2273, DOI: 10.1038/s41467-020-16109-8 (2020).

157. Ding, H., An, Y. & Shen, W. New evidence for the fluctuation characteristics of intradecadal periodic signals in length-of-day variation. *J. Geophys. Res.: Solid Earth* **126**, e2020JB020990, DOI: https://doi.org/10.1029/2020JB020990 (2021).

158. Taylor, J. The magneto-hydrodynamics of a rotating fluid and the Earth's dynamo problem. *Proc. R. Soc. A: Math. Phys. Eng. Sci.* **274**, 274–283 (1963).

159. Labbé, F., Jault, D. & Gillet, N. On magnetostrophic inertia-less waves in quasi-geostrophic models of planetary cores. *Geophys. Astrophys. Fluid Dyn.* **109**, 587–610 (2015).

160. Bizouard, C. & Gambis, D. The combined solution c04 for Earth orientation parameters consistent with international terrestrial reference frame 2005. In *Geodetic reference frames*, 265–270 (Springer, 2009).

161. Dobslaw, H., Dill, R., Grötzsch, A., Brzeziński, A. & Thomas, M. Seasonal polar motion excitation from numerical models of atmosphere, ocean, and continental hydrosphere. *J. Geophys. Res.: Solid Earth* **115** (2010).

162. Canet, E., Fournier, A. & Jault, D. Forward and adjoint quasi-geostrophic models of the geomagnetic secular variation. *J. Geophys. Res.: Solid Earth* **114**, DOI: https://doi.org/10.1029/2008JB006189 (2009).

163. Licht, A., Hulot, G., Gallet, Y. & Thébault, E. Ensembles of low degree archeomagnetic field models for the past three millennia. *Phys. Earth Planet. Interiors* **224**, 38–67, DOI: https://doi.org/10.1016/j.pepi.2013.08.007 (2013).

164. Dormy, E. & Mandea, M. Tracking geomagnetic impulses at the core–mantle boundary. *Earth and Planetary Science Letters* **237**, 300–309, DOI: https://doi.org/10.1016/j.epsl.2005.06.003 (2005).

165. Hori, K., Jones, C. A. & Teed, R. J. Slow magnetic rossby waves in the earth's core. *Geophys. Res. Lett.* **42**, 6622–6629, DOI: https://doi.org/10.1002/2015GL064733 (2015).

166. Fournier, A. *et al.* An Introduction to Data Assimilation and Predictability in Geomagnetism. *Space. Sci. Rev.* **155**, 247–291, DOI: 10.1007/s11214-010-9669-4 (2010).

167. Sanchez, S., Wicht, J. & Bärenzung, J. Predictions of the geomagnetic secular variation based on the ensemble sequential assimilation of geomagnetic field models by dynamo simulations. *Earth, Planets Space* **72**, DOI: 0.1186/s40623-020-01279-y (2020).

168. Mound, J. E., Davies, C. J., Rost, S. & Aurnou, J. Regional stratification at the top of Earth's core due to core–mantle boundary heat flux variations. *Nat. Geosci.* **12**, 575–580, DOI: 10.1038/s41561-019-0381-z (2019).

169. Hulot, G. *et al.* Nanosatellite High-Precision Magnetic Missions Enabled by Advances in a Stand-Alone Scalar/Vector Absolute Magnetometer. In *IGARSS 2018 - 2018 IEEE International Geoscience and Remote Sensing Symposium*, 6320–6323 (2018).

170. Zhang, K. A novel geomagnetic satellite constellation: Science and applications. *Earth and Planetary Physics* **7**, 4–21, DOI: 10.26464/epp2023019 (2023).

171. Alken, P. *et al.* International geomagnetic reference field: the thirteenth generation. *Earth, Planets Space* **73**, 49, DOI: 10.1186/s40623-020-01288-x (2021).

172. Langel, R. A., Estes, R. H. & Mead, G. D. Some new methods in geomagnetic field modelling applied to the 1960-1980 epoch. *J. Geomagn. Geoelectr.* **34**, 327–349 (1982).

173. Olsen, N. *et al.* Ørsted Initial Field Model. *Geophys. Res. Lett.* **27**, 3607–3610 (2000).

174. Reigber, C., Lühr, H. & Schwintzer, P. CHAMP mission status. *Adv. Space Res.* **30**, 129–134, DOI: 10.1016/S0273-1177(02)00276-4 (2002).

175. Tøffner-Clausen, L., Lesur, V., Olsen, N. & Finlay, C. C. In-flight scalar calibration and characterisation of the swarm magnetometry package. *Earth, Planets, Space* **68**, 129, DOI: 10.1186/s40623-016-0501-6 (2016).

176. Pozzo, M., Davies, C. J., Gubbins, D. & Alfè, D. Thermal and electrical conductivity of iron at Earth's core conditions. *Nature* **485**, 355–358 (2012).

177. Konôpková, Z., McWilliams, R. S., Gómez-Pérez, N. & Goncharov, A. F. Direct measurement of thermal conductivity in solid iron at planetary core conditions. *Nature* **534**, 99–101 (2016).

Box 1 : Satellite geomagnetism and the *Swarm* mission

NASA's *MAGSAT* mission in 1979-1980 provided the first globally distributed vector field measurements which allowed the large-scale magnetic field at core surface to be mapped with some confidence[96–98,172]. Starting with the launch of the Danish *Ørsted* satellite[173] in 1999 and the German *CHAMP* satellite[174] in 2000 there has been continuous monitoring of the vector magnetic field from space[91]. Since 2013 this has been carried out by ESA's three satellite *Swarm* constellation[87,88]. The three *Swarm* satellites have identical design, see Panel(a) which shows a side view of one of the *Swarm* satellites (Credit: ESA/AOES Medialab). It is 9.1 m long, launch weight was 468 kg. In the middle of a 4m boom there is a vector field magnetometer, attached by an optical bench to a star tracker that provides orientation information, and at the end of which is an absolute scalar magnetometer. Accurate location and time stamps are provided by an onboard GPS receiver. Small corrections to the raw magnetic data are carried out for known magnetic signatures of the spacecraft, including sun-driven disturbances that have been characterized in flight[175]. *Swarm* consists of a lower satellite pair, flying 150 km apart in the east-west direction that by 2022 had descended to 430 km altitude, before being slightly raised, and a third satellite at a higher altitude, around 510 km in 2022, which samples a different local time. Panel (b) shows the evolution of their altitude while panel (c) shows an example of one day data of magnetic data collected on 18th October 2018; the line segment indicates the field direction and the colours indicate its strength, created using the *Swarm* Vires data visualization tool, see https://vires.services/.

(a)

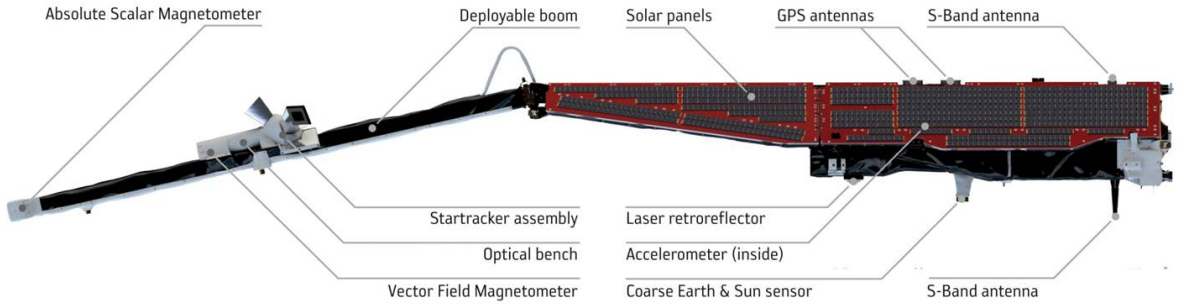

(b)

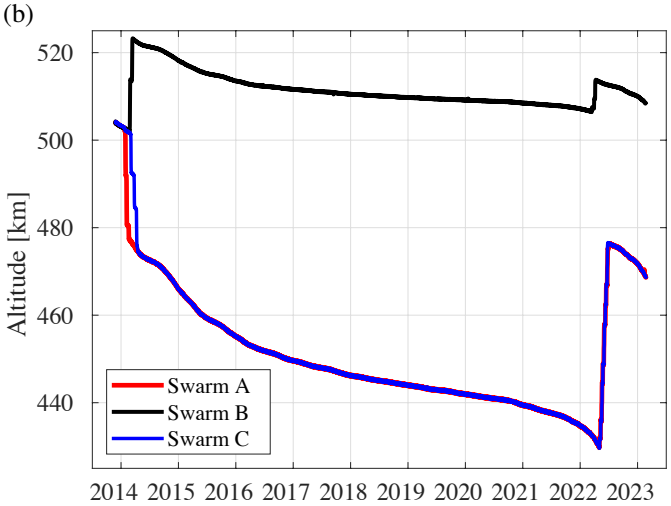

(c)

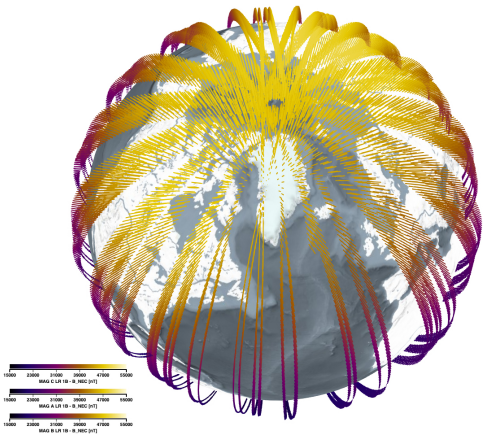

Box 2 : Numerical models of core magnetohydrodynamics

The equations governing the dynamics of Earth's fluid outer core, in a rapidly-rotating spherical shell geometry, which express the conservation of momentum, magnetic field evolution under the Magnetohydrodynamic approximation, and the transport of light material under the Boussinesq approximation, are

$$\frac{\partial \mathbf{u}}{\partial t} + (\mathbf{u}\cdot\nabla)\mathbf{u} + 2(\widehat{\mathbf{z}}\times\mathbf{u}) = -\nabla P + Ra_F C\frac{\mathbf{r}}{r_o} + (\nabla\times\mathbf{B})\times\mathbf{B}) + E\nabla^2\mathbf{u} \tag{4}$$

$$\frac{\partial \mathbf{B}}{\partial t} = \nabla\times(\mathbf{u}\times\mathbf{B}) + \frac{E}{Pr_m}\nabla^2\mathbf{B} \tag{5}$$

$$\frac{\partial C}{\partial t} + (\mathbf{u}\cdot\nabla)C = \frac{E}{Pr}\nabla^2 C + S \tag{6}$$

$$\text{with} \qquad \nabla\cdot\mathbf{u} = 0 \qquad \text{and} \qquad \nabla\cdot\mathbf{B} = 0 \tag{7}$$

where $\mathbf{u}$ is the velocity of the liquid metal, $\mathbf{B}$ is the magnetic flux density, C is the density anomaly field with a density anomaly source/sink term S, $\widehat{\mathbf{z}}$ is a unit vector along the rotation axis, time has been non-dimensionalized using the inverse of the rotation rate Ω^{-1}, velocity has been non-dimensionalized using ΩD where D is the shell thickness $r_o - r_i$, the magnetic flux density has been non-dimensionalized using $(\rho\mu_0)^{1/2}\Omega D$ where ρ is the fluid density and μ_0 is the vacuum magnetic permeability. With ν being the kinematic viscosity, κ the thermal diffusivity, η the magnetic diffusivity, g_o the gravity at the outer boundary and F the imposed mass anomaly passing the shell, the regime of the system is governed by the following non-dimensional control parameters

$$E = \frac{\nu}{\Omega D^2}, \quad Ra_F = \frac{\alpha g_o F}{4\pi\rho\Omega^3 D^4}, \quad Pr = \frac{\nu}{\kappa}, \quad Pr_m = \frac{\nu}{\eta}. \tag{8}$$

These are known respectively as the Ekman number, modified flux Rayleigh Number, Prandtl number and magnetic Prandtl number. In Earth's core their values are estimated to respectively 10^{-15}, 10^{-12}, 0.1-1 and 10^{-6}. The fluid has been assumed incompressible. Standard boundary conditions[18] involve impenetrable no-slip and electrically insulating boundaries for the velocity and magnetic fields, and a prescribed temperature difference between the inner and outer boundaries. Numerical solutions are obtained by discretisation of these partial differential equations usually by means of spherical harmonics horizontally and finite differences or Chebyshev polynomials in the radial direction, and time-stepping using mixed implicit-explicit schemes to handle the diffusive and linear, and respectively the nonlinear terms.

In an effort to reach a geophysically relevant regime, the simulations presented here in Figs. 2 and 4 use a slightly modified setup[17,27,80]. They minimise the viscous boundary layer by adopting stress-free mechanical conditions, model the effects of an electrically conducting inner core and a conducting basal layer in the mantle, and impose a convective mass anomaly flux at the inner and outer boundaries rather than prescribing a fixed temperature difference. A large-eddy simulation strategy[80] is adopted based on a proposed downscale transfer of energy by magnetic turbulence under the QG-MAC force balance. This involves hydrodynamic turbulence below the scale of magnetic dissipation being neglected, since it is argued to be responsible for a negligible part of energy transfers and dissipation, by numerically enhancing the viscous and thermo-chemical diffusivities $\nu_{\text{eff}}, \kappa_{\text{eff}}$ above a given spherical harmonic order ℓ_h according to:

$$(\nu_{\text{eff}}, \kappa_{\text{eff}}) = (\nu, \kappa) \text{ for } \ell < \ell_h, \tag{9}$$

$$(\nu_{\text{eff}}, \kappa_{\text{eff}}) = (\nu, \kappa)\, q_h^{(\ell-\ell_h)} \text{ for } \ell \geq \ell_h, \tag{10}$$

with $\ell_h = 30$ and q_h=1.09 for the simulations presented here. On large scales this allows parameter values $E = 3\times10^{-10}, Ra_F = 2.7\times10^{-10}, P_m = 7.9\times10^{-3}, Pr = 1$ to be reached and ratios of relevant time scales (Table 1) to approach those expected in Earth's core.

Table 1 : Key timescales of core dynamics

	Thermal diffusion $\tau_\kappa = D^2/\kappa$	Magnetic diffusion $\tau_\eta = D^2/\eta$	Overturn $\tau_U = D/U$	Alfvén $\tau_A = \sqrt{\rho\mu_0}D/B$	Rotational $2\pi\tau_\Omega = 2\pi/\Omega$
Earth's core	$5\times10^9 - 3\times10^{11}$ yr	$5\times10^4 - 3\times10^5$ yr	≈ 130 yr	≈ 2 yr	1 day
Advanced simulation[27]	$\approx 10^7$ yr	$\approx 10^5$ yr	≈ 130 yr	≈ 6 yr	≈ 10 days

Key time scales relevant to magnetic diffusion, the slow convective overturn, the rapid Alfvén wave propagation, and the imposition of the rotational constraints in Earth's core. Estimates for Earth's core are obtained with the root-mean-squared velocity inside the core[5,62] $U = 17$ km/yr, root-mean-squared magnetic field intensity[22] $B = 4$ mT, $\rho = 11000$ kg/m^3, $D = 2260$ km, $\mu = 4\pi\times10^{-7}$ H/m, $\Omega = 7.29\times10^{-5}$ 1/s, and a range $\eta = 0.5 - 3$ m^2/s for magnetic diffusivity[176,177].

Glossary terms

Alfvén waves: Waves arising in an electrically conducting fluid due to the interplay of fluid inertia and magnetic (Lorentz) forces.

Frozen flux Approximation: Under this approximation changes in the magnetic field are produced by advection and stretching of a moving conductor and magnetic diffusion effects are neglected.

High latitude jet: a localized region of high fluid velocity located under Alaska and Siberia that is associated with a distinctive pattern of magnetic field change at high northern latitudes. Usually considered to be part of the planetary gyre.

Hydromagnetic waves: Waves that can occur in electrically conducting fluids in the presence of a strong magnetic field. Their properties depend on the force balance in the system. Alfvén waves are the simplest example, other examples include Magneto-Coriolis (MC) and Magneto-Archimedes-Coriolis (MAC) waves.

Inner core tangent cylinder: An imaginary cylinder parallel to Earth's rotation axis and just touching the inner core in the equatorial plane. Acts as a natural dynamical barrier to columnar flows so that, to a large extent, the regions above and below the inner core, and that outside the tangent cylinder, are dynamically separated.

Magnetohydrodynamics: Combination of hydrodynamics, as described by the Navier-Stokes equation, and electrodynamics under the quasi-static approximation as described by the magnetic induction equation. Sometimes also called hydromagnetics.

Magneto-Coriolis (MC) waves: waves in rapidly rotating, electrically conducting fluids where the force balance is between magnetic and Coriolis effects, with inertia playing a negligible role. Sometimes also called magnetostrophic waves.

Magneto-Archimedes-Coriolis (MAC) balance: A dynamical balance between Magnetic (Lorentz), Archimedes (Buoyancy) and Coriolis forces that is thought to be important for the core flow. The scenario when rotation dominates at leading order, and this balance holds at the next order and involves only the remaining (ageostrophic) part of the Coriolis force, is known as a QG-MAC balance - see equation (2).

Planetary gyre: The basic anticyclonic circulation of the liquid metal in the outer core that is of planetary scale and eccentric (offset) from the rotation axis. It flows westwards at mid and low latitudes under the Atlantic hemisphere, polewards under the Americas, westwards under Alaska and Siberia at high latitudes and returns equatorward under eastern longitudes. Believed to be largely equatorially symmetric but with some localized departures.

Quasi-geostrophy (QG): An approximate leading order balance in the Navier-Stokes equation between the Coriolis force and the pressure gradient. Occurs in rapidly rotating fluids and leads to approximately columnar flow structures. Departures from geostrophy controls the dynamics of the columnar structures.

Swarm satellite mission: Trio of low-Earth-orbit satellites launched by ESA in 2013 to survey Earth's magnetic field.

Torsional waves: Special Alfvén waves (see above) that can occur in rapidly rotating fluids which are axisymmetric, equatorially symmetric, and propagate in the cylindrical radial direction.

Acknowledgements

The authors thank Richard Holme and three anonymous reviewers for constructive comments. We wish to thank ESA for the prompt availability of Swarm L1b data. The staff of the geomagnetic observatories and INTERMAGNET are thanked for supplying high-quality observatory data. This work was supported by ESA under the framework of EO Science for Society, through contract 4000127193/19/NL/IA (Swarm+4D Deep Earth: Core). The authors would also like to thank the Isaac Newton Institute for Mathematical Sciences, Cambridge, for support and hospitality during the programme DYT2 during which final work on this paper was carried out, supported by EPSRC grant no EP/R014604/1.

Competing interests

None.

Publisher's note